VTT Technical Research Centre of Finland

Impact of power-to-gas on the cost and design of the future low-carbon urban energy system

Ikäheimo, Jussi; Weiss, Robert; Kiviluoma, Juha; Pursiheimo, Esa; Lindroos, Tomi J.

Link to publication

Please cite the original version:
Ikäheimo, J., Weiss, R., Kiviluoma, J., Pursiheimo, E., & Lindroos, T. J. (2022). Impact of power-to-gas on the cost and design of the future low-carbon urban energy system. *Applied Energy*, *305*, [117713]. https://doi.org/10.1016/j.apenergy.2021.117713

Impact of power-to-gas on the cost and design of the future low-carbon urban energy system

Jussi Ikäheimo [*], Robert Weiss, Juha Kiviluoma, Esa Pursiheimo, Tomi J. Lindroos

Smart Energy and Built Environment, VTT Technical Research Centre of Finland Ltd, Tekniikantie 21, FI-02044 VTT Espoo, Finland

ABSTRACT

Power-to-gas technology has been proposed as one component for future energy systems facing decarbonization targets. This paper presents a power-to-gas focused open optimization model for studying cost efficient design and operation of future urban energy system. The model is able to distinguish the benefits of different configurations of power-to-gas by modelling several energy vectors, including electricity, heating, and cooling alongside with different plant components. The usefulness of the built multi-vector model is illustrated by a case study where the benefits of power-to-gas are studied in the context of a medium-sized Nordic city. The results show that the city is able to reach carbon neutrality with the help of power-to-gas. Power-to-gas provides cost savings by reducing the need of heat storages and transmission capacity. The savings are greatest when the emission reduction goal is high and transmission capacity expansion is expensive. Direct air capture appears as the superior carbon dioxide source when compared to post combustion capture from flue gases due to costs and annual availability. The case study shows no economic benefit for distributed power-to-gas.

1. Introduction

To limit global warming below $1.5\,°C$, carbon dioxide (CO_2) emissions should decline by 40%–60% by 2030 and reach net zero close to 2050 [1]. To reach this target, installation of massive amount of variable renewable energy (VRE) generation, mainly wind and solar, will be essential [2]. Fossil carbon needs to be removed from all energy sectors including heating, cooling, and transport while at the same time power system needs to cope with a large variability of generation. Chemical storage of electrical energy has been proposed as a key option in tackling the challenge [3]. Power-to-gas (P2G), which refers to production of both hydrogen and methane using electrical energy, has been suggested as an option for chemical energy storage [4]. Synthetic methane and up to some extent, hydrogen, can substitute natural gas in existing gas networks. In recent years, a great number of studies have been published about the role of P2G in national and continental energy systems [5].

In addition to international emission reduction targets, targets have been also set on local level. For example, the Covenant of Mayors [6] urges cities to pursue energy efficiency and emission reductions. Energy system analysis which focuses on single city can help to reach the targets in a cost-efficient way by providing additional information on local conditions and operation environment. The fact that cities' share of the global energy demand and carbon emissions is approaching 80% [7] also advocates the need for city level analyses. European

district heating (DH) and cooling systems, which are major energy consumers in cities, are still mainly based on fossil fuels [8], most commonly on natural gas [9]. From the energy system studies point of view, analysing local systems is attractive because it allows more attention to detail which would, because of computational limitations, be beyond reach in national or continental analyses. The presence of energy storages, including chemical energy storages, can significantly increase the system optimization complexity [10].

While renewable energy integration in urban energy systems has been widely studied [11], the contribution of P2G on the security of supply, carbon emissions and economic affordability in urban energy systems has not yet been fully addressed. Analysing the role of P2G on the city level is interesting because of its interactions with other energy vectors [12]. Especially in Nordic countries district heating networks are normally present and allow cost-efficient exploitation of waste heat from large point sources. P2G produces waste heat and benefits from economies of scale. P2G needs CO_2 as input, which is currently produced in large quantities by power and heating plants in cities [13]. If on the other hand CO_2 is extracted from ambient air, district heating may serve as an affordable heat source for the process. District cooling is a relatively new technology, which can act as a source of excess heat or a sink of cooling. Cities are also major electricity consumers and it is important to consider also the effect of grid restrictions on P2G [14].

Nomenclature

Abbreviations

ASHP	Air-source heat pump
BESS	Battery electric storage system
CCGT	Combined cycle gas turbine
CCUS	Carbon capture, utilization and storage
CHP	Combined heat and power
COP	Coefficient of performance
DAC	Direct air capture
DC	Direct current
DGSHP	Deep ground-source heat pump
DH	District heating
EV	Electric vehicle
HHV	Higher heating value
HP	Heat pump
HP	High pressure
IP	Intermediate pressure
LP	Low pressure
MILP	Mixed integer linear programming
P2G	Power-to-gas
P2H	Power-to-heat
PCC	Post combustion capture
PEMEL	Proton exchange membrane electrolysis
PV	Photovoltaic
SMR	Methane steam reforming
SNG	Synthetic natural gas
SOFC	Solid oxide fuel cell
VRE	Variable renewable electricity
WWHP	Waste water heat pump

Indices

f	Fuel
g	Technology
i	Step in electricity market supply curve
j	Step in hydrogen production function
t	Time

Symbols

α_g	Capital recovery factor of technology g
α_{grid}	Capital recovery factor of grid investments
β_{eff}	ASHP efficiency function coefficients
β_P	ASHP heat output function coefficients
η_{hp}	Heat pump coefficient of performance
γ	Heat capacity ratio
λ_{hyd}	Maximum admissible hydrogen concentration in gas grid
ψ	Exergy efficiency
θ_j	Maximum operation point of component j of hydrogen production
C^{LEV}	Levelized total annual cost
C_g^E	Total emission cost of technology g
$C_g^{FOM,base}$	Total fixed operation and maintenance cost of technology g without grid demand charges
C_g^{FOM}	Total fixed operation and maintenance cost of technology g
C_g^F	Total fuel cost of technology g
$C_g^{INV,base}$	Total investment cost of technology g without grid connection costs
C_g^{INV}	Total investment cost of technology g
$C_g^{startup}$	Total start-up cost of technology g
C_g^{VOM}	Total variable operation and maintenance cost of technology g
c_{dist}^{FOM}	Distribution grid unit demand charge
c_{dist}^{INV}	Grid connection unit investment cost
c_{dist}^{VOM}	Energy dependent distribution fee
$c_{em,i}$	Step increase in electricity market price
c_{em}	Electricity market price
$c_{g,f}^F$	Unit fuel cost of fuel f for technology g
$c_{grid,HV}$	Specific cost of transmission grid reinforcement
$c_{grid,LV}$	Specific cost of distribution grid reinforcement
C_{grid}^{INV}	Total electrical grid investment
J	Number of piecewise approximation components in hydrogen production
$K_{grid,HV}^0$	Initial capacity of the transmission grid connection in terms of electrical capacity
$K_{grid,HV}^e$	Investment into electrical transmission grid reinforcement in terms of electrical capacity
$K_{grid,LV}^e$	Investment into electrical distribution grid reinforcement in terms of electrical capacity
K_g^e	Investment into technology g in terms of electrical capacity
L_g	Economic lifetime of technology g
n	Molar flow rate
P	Power
p	Pressure
P_j	Component in electrolysis input power
Q	Thermal power
Q_0	Nameplate thermal power
R	Specific gas constant
r	Discount rate
T_{amb}	Ambient air temperature
$T_{sink,in}$	Heat pump condenser intake temperature
$T_{sink,out}$	Heat pump delivery temperature
T_s	District heating supply temperature
u_{gas}	Relative annual gas usage reduction
$V^{hyd,max}$	Maximum hydrogen production by electrolysis
V_{exp}^{gas}	Gas export from the model region
$V_{g,f}^{F,cons}$	Fuel consumption of fuel f by technology g
$V_{imp,i}^{elec}$	Component of electricity import to the model region
V_{imp}^{elec}	Electricity import to the model region
V_{imp}^{gas}	Gas import to the model region
V_j^{hyd}	Piecewise approximation component of hydrogen production
W_{hp}	Mechanical power consumed by heat pump

Wider gas grids are normally found in cities, which allows emission reductions throughout the local energy system by distributing synthetic natural gas (SNG) in the gas grid [15].

1.1. Literature review and contributions

The analysis of future scenarios where novel technologies become available is usually performed with the aid of an energy system model. As there is a trade-off between model features and computational feasibility, one is advised to select a suitable model for each application [16]. We need a model which can consider several energy vectors to analyse the contribution of P2G in urban energy systems . We can thus approach the research question from two directions. Firstly there are studies concentrating on planning and optimization of multi-vector energy systems. Secondly, there are several categories of studies focusing on P2G [5]. These include also cost optimization studies. From the point of view of the current study, the intersection of these two lines of research is most interesting.

A number of studies which pay attention to multiple energy vectors and include also P2G have been published. These differ in terms of the energy vectors and technologies included, availability of options to import and export, and the extent of optimization. Some studies employ simulation approach rather than cost optimization. Study [15] simulated the use of electric and gas driven heat pumps (HP), combined heat and power (CHP), and P2G to satisfy heat demand at three different temperature levels in three example cities. P2G was only used to convert excess VRE to gas. Study [8] investigated the supply of electricity and district heat by VRE in a Finnish rural town, using P2G for reaching net zero consumption of natural gas. Using rule-based dispatch it was determined that electrolysis of 1.2 MW capacity was needed to reach zero emissions, which is approximately $1/6$ of the peak DH load. In the analysis [17] the capacities of different conversion technologies were given as input and their effect was investigated. The heat sector was included with given heat price. The authors found that P2G was not able to reduce the average cost of electricity unless very low capital cost was assumed.

Study [18] used rule-based dispatch and capacity optimization to study the effect of increasing share of renewable electricity in the Berlin–Brandenburg region. P2G entered the cost-optimal capacity mix at very high renewable electricity shares. However, the heat sector was not included. Conversely study [19] performed only dispatch optimization on a system comprising power, heat, and gas vectors. Genetic algorithm was applied as solution method to take account also transmission constraints.

Some studies carry out both system planning (i.e. optimize plant capacities) and operational optimization. The German Rheinland-Palatinate region was considered an electrical island with 100% renewable energy penetration in study [20]. The heat sector was included as sink with exogenous price of heat. P2G entered the cost optimal system when its investment cost decreased below $2500 €/kW$. Conversely in [21] limits for renewable energy share were not set but the effect of taxes and natural gas price on P2G and power-to-heat (P2H) profitability. Price of electricity was externally given. The effect of gas price on the P2G, which could exploit CO_2 from a biomass combined heat and power (CHP) plant, was studied in [22]. In that study the model city could also trade with external power market. Study [23] considered heat and electricity vectors but only a limited number of technologies. In that study the objective was not minimization of cost but minimization of emissions. Multiple energy vectors were included in study [24] but the heat sector was missing.

A group of studies includes optimization of plant capacities and multiple energy vectors but take the perspective of a single plant. Study [25] created a process model for the P2G plant, which was then linearized for the purpose of optimization against electricity market. The study paid particular attention to oxygen revenues and very high oxygen prices were also considered. Study [26] studied the optimal sizing of a building-scale P2G plant producing both methane and oxygen. Methane and oxygen could be consumed in an oxyfuel boiler with carbon capture from fluegases, producing heat for local consumption.

As mentioned, another stream of literature concerns optimal system planning and scheduling in multienergy systems. In these studies, P2G is not normally modelled but could possibly be added to the models with reasonable amount of work. Study [27] developed a mixed integer quadratic programming model for simultaneous electricity and cooling production and applied it to a group of office buildings. Study [28] applied the energy hub concept to a system comprising electricity, gas and heat flows and solved the energy cost minimization problem using gravitational search algorithm. Review [29] found that the interaction between gas and electricity grids has been widely studied in optimal planning models but heat networks are much less commonly included. Furthermore, the review suggested economic value of energy systems integration as well as the optimal level of integration (transmission or distribution) as future research topics.

P2G can produce both methane and hydrogen. In existing literature normally only one product is analysed. Hydrogen can be fed into existing gas networks in certain quantity; varying concentration limits have been set in different countries. In study [30] it was envisioned how to convert of the gas distribution of one whole city from natural gas to hydrogen. In that study methane steam reforming (SMR), which needs to be accompanied by carbon sequestration, was considered as the main hydrogen production technology. Electrolysis was given only an augmenting role due to high cost of electricity and large land foot print of carbon-free electrical generation.

In this study we perform planning and dispatch optimization for an urban multi-energy system of the near future. We concentrate on economic affordability and examine if P2G can contribute to reduction of costs when emission reductions are pursued. The novelty of the paper lies in an unique combination of modelling features. We seek to provide cost optimal solutions by optimizing both capacity investments and the day-to-day operation of the system. Compared to most previous studies, we consider cost optimal ways of fulfilling heat, cooling, gas and electrical demand. A variety of technologies for generation of electricity, heat and cooling are included. Unlike in most studies, where the attention has been given to the rest of the system [5], we also touch upon the process design of the P2G plant by modelling several plant components separately. P2G needs CO_2 and we consider two different options for CO_2 supply: direct air capture and post-combustion capture from flue gases. We also consider both hydrogen and methane products of P2G. By-products waste heat and oxygen are also considered.

We also consider the significance of the electrical grid and other energy grids from several viewpoints. One of the trends of the energy sector is the emergence of distributed energy resources. We include technologies such as distributed P2G and electric vehicles, which may also provide flexibility and help to reduce emissions. The trade-offs between electrical grid reinforcement and P2G are studied both for centralized and distributed P2G. We apply the model to a Nordic city and clearly show the economic benefits of P2G at different levels of ambition of emission reductions.. The model is also made available to the research community.

1.2. Paper organization

The analysis is performed by building and running an energy system planning and scheduling model. In Section 2.2 the model is introduced and balancing the computational burden and model detail is discussed. The modelling of P2G and other relevant conversion and storage technologies are explained in Section 2.3. In addition, we justify the choices of relevant technical and financial parameters. Section 2.4 defines a case study to produce practical results and illustrate functioning of the model. Results of the case study are shown in Section 3 and the results are discussed in Section 4. Finally, Section 5 concludes the insights of the paper.

2. Materials and methods

2.1. Modelling the urban area

Fig. 1 shows the schematic layout of the conversion units and flows of energy vectors in the model. To avoid cluttering of figure, some details of the system are presented later in Section 2.3. The four energy vectors modelled are electricity, heat, cooling, gas, and hydrogen. Electricity can be produced by combined cycle gas turbine (CCGT) combined heat and power (CHP) plant, gas engines or turbines, solar PV, and wind turbines. Short-term storage is possible with battery electric storage system (BESS). District heat can be produced by the CHP plant, gas and electric boilers, and different types of heat pumps. Hydrogen can be produced by electrolysis plant, stored and fed to the methanation plant or directly to gas grid. CO_2 for methanation is captured from CHP flue gases at post combustion capture plant or directly from ambient air. Methanation produces SNG which substitutes fossil natural gas. District cooling can be produced by heat pumps, compression chillers or free cooling using seawater. In addition, heat and cooling are available as byproducts of the power-to-gas process. District heating and cooling networks are local to the city, but electricity and natural gas can be imported from or exported to the national transmission grids.

2.2. Optimization

The optimization problem considered in this work can be stated in concise form as follows. Given

- Demand profiles and weather data
- Available technologies, their costs, performance data and operational constraints
- Reduction goal of fossil fuel usage

Determine:

- Selection of technologies to invest in
- Operation profiles of different units
- Management strategy of the storage systems
- Energy import and export profiles
- Grid reinforcement investments

This is done subject to:

- Technical constraints of conversion units
- Fulfilling demand of electricity, heat and cooling

The open-source Backbone modelling framework [31] was chosen as the optimization framework because of its adaptability and capability of including multiple energy sectors. Backbone allows the specification of both investment (generation expansion planning) and short-term scheduling models (also called production cost models). However, unlike in traditional generation expansion and scheduling models [32], also other flows besides electricity can be modelled.

As the first step in the optimization process, the investment model is used to determine the optimal capacities of different plant components (conversion units in Backbone model terminology). This is unlike e.g. the method used by Mazzoni [27] where the plant capacities and their operation is optimized simultaneously. The benefit of using separate models is that the emphasis of modelling simplifications can be set separately so that it serves the purposes of each model. For example, when performing scheduling optimization, the emphasis is normally in the short-term horizon of few days. The investment model must consider a longer horizon but this would in our case be computationally intractable using high temporal resolution.

Several methods exist for reducing the number of time steps in the model without sacrificing accuracy proportionally. One approach is to select representative slices of the original time series [33]. Representative slices are subsets of the original time span which is considered in optimization. One or more slices can be specified. The slices are normally not adjacent and rules must specify how state variables (such as state of charge of storages) behave upon the transition from one slice to the next. Some studies assume cyclic constraints which do not allow change in the state of charge over a slice [34]. The rules applied in Backbone for state variables are similar to the ones presented in [35]. However, they are simplified in the respect that there is not explicit allocation of every time step of the original time span into certain representative slice.

The length and number of representative slices must be chosen to balance the computational load of the investment model and its accuracy. Studies [33,36] found that the accuracy of results (in terms of total cost deviation) generally increases as function of the temporal extent of the representative slices. Study [33] reached good results with 35 representative days, divided into five slices. Study [36] reached good results already with 28 representative days in a power-only model and suggested that comparable temporal extent reduction assumptions may be justified for similar models. Concerning the computation time, both the current study and study [36] found that it increases rapidly as more days are added. Consequently, in this study 40 representative days were chosen and they were divided into four slices. The representative slices were selected from a full year time series using random sampling as explained in [33]. These slices normally do not include extreme periods. There is no general consensus about the best way to select slices for extreme periods in multi-vector energy systems [37]. In this study, a slice was selected from the period of peak heat and electrical load.

There are several attribute time series which one may consider in the sampling process of a multi-vector model. Heat demand is clearly an important attribute when heat must be produced within the system [38]. The same can be said about cooling demand, however, as it is inversely correlated with heat demand, it was not included as separate time series. From the point of view of P2G and many heat production technologies electricity price should be modelled accurately. Thus four attributes were used in the sampling: electricity price, heat demand and wind and solar PV capacity factors. If the results showed that local VRE is insignificant, a second sampling round was done with only electricity price and heat demand profiles.

As shown in Fig. 2, the resulting portfolio of unit capacities is fed as input to the scheduling model. Scheduling models often consider rolling time horizons between 24 h to 48 h [32]. Computation time, which may increase up to exponential rate with the number of time steps [36], limits the horizon [39]. In our model the time horizon could be increased considerably because Backbone allows variable time steps in optimization. We specify optimization horizon of one year, where the time step gradually increases from one hour (up to 24-hour horizon) to one month. The long horizon helps the scheduling optimization to take account annual constraints such as maximum annual usage of fossil natural gas. To create results with hourly time resolution, the scheduling model is run multiple times with rolling horizon so that one year is covered.

2.2.1. Objective function

In this study, the objective is minimization of the total annual cost of the system, as the inadequacy of the widespread levelized cost of electricity (LCOE) metric as objective has been recognized [40]. The total annual cost includes capital costs as well as fixed and variable annual costs of conversion units and grid connections. The total annual cost is calculated as

$$C^{LEV} = \sum_g \left(\alpha_g C_g^{INV} + C_g^{FOM} + C_g^{VOM} + C_g^{startup} + C_g^E \right)$$
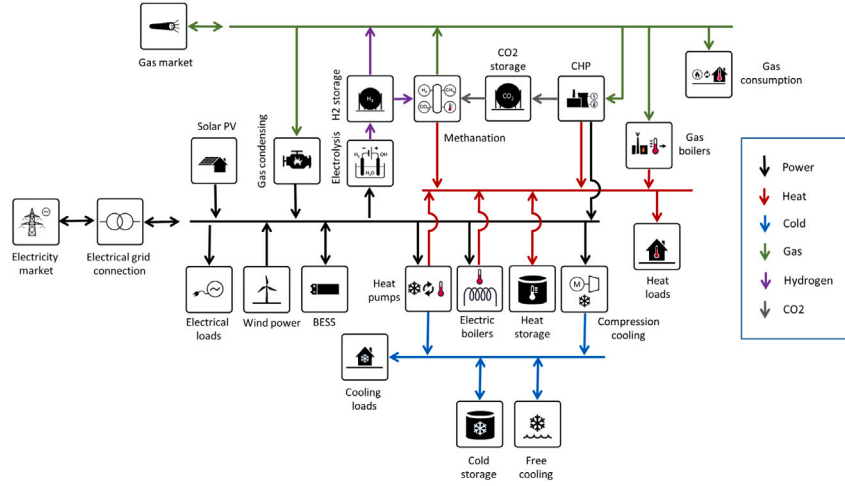$$+ \sum_g \sum_f C_{g,f}^F + \alpha_{grid} C_{grid}^{INV} \tag{1}$$

Fig. 1. Overall layout of the city energy system model with conversion unit types and flows of energy and gases. For simplicity some details have been left out of this diagram and are presented in other figures.
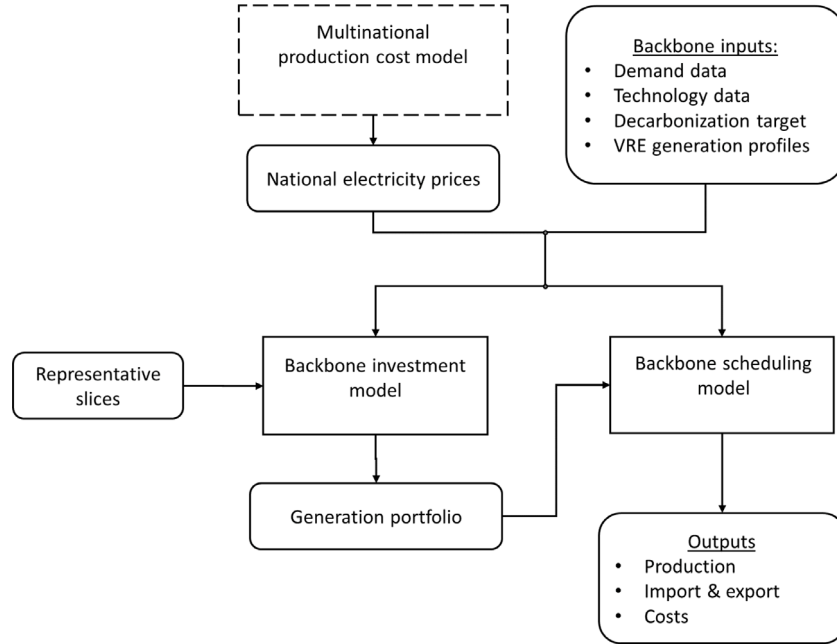

Fig. 2. Overall flowchart of the modelling workflow. Two different models (shown inside rectangles) were used in a soft-linked scheme to obtain the results.

where C_g^{INV}, C_g^{FOM}, C_g^{VOM}, $C_g^{startup}$, $C_{g,f}^{F}$ and C_g^{E} are capital costs, annual fixed operation and maintenance costs, annual variable operation and maintenance costs, start-up costs, fuel costs, and emission costs for conversion unit g using fuel f, respectively. C_{grid}^{INV} is the total amount of grid reinforcement investments. The capital recovery factor [41]

$$\alpha_g = \frac{r(1+r)^{L_g}}{(1+r)^{L_g} - 1} \qquad (2)$$

where L_g is the economic lifetime of unit g and r is the discount rate. α_{grid} is the corresponding factor for grid investments. Here fuels are only those energy vectors which have an external cost, such as electricity, fossil gas, and biogas. Only CO_2 emissions are considered and their only source is gas (fossil gas or SNG). Emissions of imported electricity are not accounted for. This is justified by the small amount of fossil based generation in the projected electricity production scenario [42]. As result of the electricity market functioning, the emission cost is also included in the import electricity price. Notice that there are no separate terms for fuel import and export in Eq. (1): the model includes

special units which are responsible for importing and exporting fuels and these costs are thus included in C_g^{F}.

2.2.2. Constraints

Besides technical constraints at each conversion plant, the model contains system-wide constraints. Capacity investments are limited by land use considerations. Electricity, heating and cooling demands must be fulfilled at all times. Electricity may be imported and exported subject to limit in the grid connection capacity. While the connection to the gas transmission grid has also certain capacity, the major constraint is the annual fossil gas use limit. The net fossil gas consumption is first calculated when no constraints are set as in Eq. (3).

$$U_{gas} = \sum_t \left(V_{imp}^{*gas}(t) - V_{exp}^{*gas}(t) \right) \qquad (3)$$

where $V_{imp}^{*gas}(t)$ is gas import to the model region and $V_{exp}^{*gas}(t)$ is gas export from the model region at time t. The asterisk refers to the result value from the optimization model. We can now define a coefficient

which states the relative net usage goal u_{gas} of fossil gas. Gas usage constraint is then set as in Eq. (4).

$$\sum_t \left(V_{imp}^{gas}(t) - V_{exp}^{gas}(t) \right) \leq (1 - u_{gas}) U_{gas} \tag{4}$$

2.2.3. Electricity supply

As the geographical scope of the built Backbone multi-energy model is one city, electricity markets are exogenous to the model. The power market was modelled using a separate production cost model as described in [43]. The marginal cost of electricity $c_{em}(t)$, which in perfectly competitive markets should approach the market price, was fed as input to the Backbone model. The time-dependent elasticity of the market price cannot be calculated exactly in the model framework. As an approximation we assume a time-invariant linear dependency of the market price of total demand in the market area. Considering that the power market is a uniform price auction, a single large consumer also faces linear dependency of her marginal electricity cost of her demand. To keep our model within the class of mixed integer linear programming (MILP) models, the price increase is approximated with a stepwise curve, described as below:

$$V_{imp}^{elec}(t) = \sum_i V_{imp,i}^{elec}(t) \tag{5}$$

$$V_{imp,i}^{elec}(t) \leq V_{imp,i}^{elec,max} \tag{6}$$

$$C_{imp}^{elec}(t) = \sum_i \left[\left(c_{em}(t) + c_{em,i}^{add} \right) V_{imp,i}^{elec}(t) \right] \tag{7}$$

where $V_{imp}^{elec}(t)$ is the imported amount of electricity and $C_{imp}^{elec}(t)$ is its cost. $c_{em}(t)$ is the market price. $V_{imp,i}^{elec,max}$ and $c_{em,i}^{add}$ are constant terms describing the elasticity of price when import increases. Electricity export is also possible but because of its small significance in the studied case, the price elasticity was not implemented for exports.

To physically access the power market, transmission capacity must be present. Depending on the scenario, transmission capacity was specified exogenously as $K_{grid,HV}^0$ or was subject to investment. Transmission constraints within the city were not considered. However, to study the effect of distributed resources, a separate low voltage (LV) bus was created. Several technologies connect to the LV bus: distributed PV, EV and distributed P2G. Dimensioning of the grid connection between the main city electrical bus and the LV bus was a responsibility of the investment model; distributed technologies can thus contribute to deferral of the grid investment. The grid investment costs are calculated as

$$C_{grid}^{INV} = c_{grid,HV}^{INV} K_{grid,HV} + c_{grid,LV}^{INV} K_{grid,LV} \tag{8}$$

where $c_{grid,HV}^{INV}$ is the unit cost of grid reinforcement investments in the transmission capacity to the national grid and $K_{grid,HV}$ is the invested capacity (see Fig. 3).

Distribution grid charges for major electricity consuming units were modelled using three components, reflecting the existing tariff structure. Connection fees were included in plant investment costs C_g^{INV}:

$$C_g^{INV} = C_g^{INV,base} + c_{dist}^{INV} K_g^e \tag{9}$$

where K_g^e is the electrical capacity of the unit and c_{dist}^{INV} is the connection fee to distribution network. Capacity-based demand charge, applied in many European countries [44], was included in the fixed annual costs of each plant. This was also charged based on the installed electrical capacity of the plant:

$$C_g^{FOM} = C_g^{FOM,base} + c_{dist}^{FOM} K_g^e \tag{10}$$

where c_{dist}^{FOM} is the demand charge per unit of capacity. The third component was electricity distribution energy fee, which were collected based on the consumed electricity. Electricity is considered as fuel in the model and the total distribution energy fees are thus calculated as

$$C_{g,f}^F = \sum_t c_{g,f}^F(t) V_{g,f}^{F,cons}(t) \tag{11}$$

$$c_{g,f}^F(t) = c_{g,f}^{F,base} + c_{dist}^{VOM}(t), \quad f \in \{ electricity \} \tag{12}$$

and $c_{g,f}^F(t)$ is the specific fuel cost of fuel f at time t, $V_{g,f}^{F,cons}(t)$ is the consumption of fuel f by unit g, and $c_{dist}^{VOM}(t)$ is the distribution energy fee.

2.3. Modelling of conversion units

2.3.1. Electrolysis

Electrolysis is the most mature hydrogen production technology which can use renewable electricity as input [45]. Requirements for electrolysis in P2G applications include ability for dynamic behaviour and low lifetime cost [13]. While alkaline electrolysis is currently the most commercialized technology, an expert elicitation study [46] found that proton exchange membrane electrolysis (PEMEL) was estimated to be most suitable technology for production of renewable hydrogen into the natural gas grid in 2030. Böhm et al. [47] estimated that PEMEL will take over alkaline electrolysis in market share in 2030's. Solid oxide electrolyser cell systems have so far mainly been developed on laboratory and pilot scale. Consequently in this study PEMEL has been modelled.

It is important to distinguish the different definitions of conversion efficiency [48]. The scope of the system for which efficiency is calculated may include the electrolysis stack, auxiliaries such as rectifiers and pumps, compressors for the product gas. The present day efficiency of PEMEL system without external compression, was stated as $5.0\,kWh/Nm^3$ to $6.5\,kWh/Nm^3$ ($\eta_{HHV} = 55\%$–71%) [48]. For 2030 $4.2\,kWh/Nm^3$ to $5.6\,kWh/Nm^3$ ($\eta_{HHV} = 63\%$–84%) [46], $4.0\,kWh/Nm^3$ to $4.8\,kWh/Nm^3$ ($\eta_{HHV} = 74\%$–90%) [49] and $4.72\,kWh/Nm^3$ ($\eta_{HHV} = 75\%$) [50] was predicted. It has to be noted that this is the efficiency of a new device and it will decrease with ageing.

In part load operation efficiency clearly increases because of reduction of overpotentials which impact the cell voltage [51]. For example the efficiency of a 6 MW PEMEL in Energiepark Mainz rises from 65% to 76% when operated at 27% part load [48]. Nonlinear characteristics such as plant efficiencies are often linearized but reducing the efficiency term to a constant can lead to high degree of inaccuracy [39]. Here we adopt piece-wise linear approximation of the electrolysis production function. Unlike argued in [39], the piece-wise efficiency approximation does not require fixing the electrolysis capacity exogenously. In the Backbone model framework, the varying efficiency can be described with piece-wise linear approximation using the incremental heat rate presentation [31]. This involves presenting input power P and hydrogen mass flow V^{hyd} as sum of J components:

$$P = \sum_{j=1}^J P_j, \tag{13}$$

$$V^{hyd} = \sum_{j=1}^J V_j^{hyd} \tag{14}$$

The component variables P_j and V_j^{hyd} are then tied by efficiencies and limited by operating points θ_j:

$$P_j = V_j^{hyd} \times \eta_j^{hyd} \quad \forall j \in [1, J] \tag{15}$$

$$V_j^{hyd} \leq \left(\theta_j - \theta_{j-1} \right) V^{hyd,max} \quad \forall j \in [1, J] \tag{16}$$

The coefficients η_j^{hyd} were chosen at equal intervals so that the minimum and maximum efficiencies are equal to the chosen values (see Table 3). The total efficiency can be increased by exploiting the generated heat and it can exceed 90% (HHV) when waste heat is exploited [52]. 15% of input energy was assumed to be available as heat [53]. As explained in Section 2.3.8, a heat pump must be used to lift the temperature to match DH supply.

Investment cost estimates ranging from $400\,€/kW$ to $950\,€/kW$ [52] and $500\,€/kW$ to $1300\,€/kW$ [46] have been presented for PEMEL for
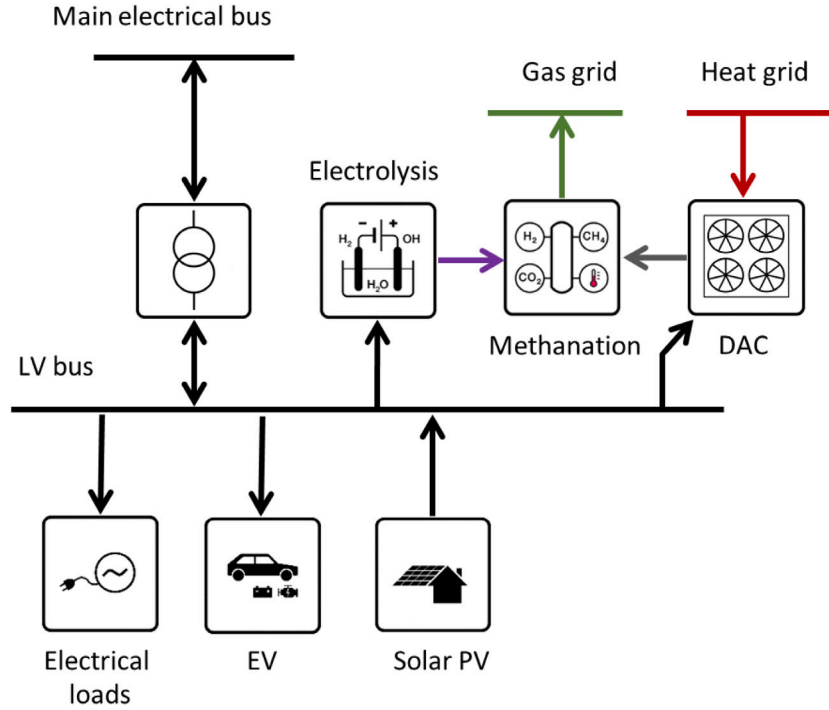
Fig. 3. Layout of the low-voltage bus of the city energy system model. The low-voltage bus was connected to the main electrical bus via transformer whose capacity is set by the variable $K_{grid,LV}$.

year 2030 . In this study $600 \in /kW$ was used for $C_g^{INV,base}$. The electrolysis stack, which accounts for 40% of the initial investment [54], needs periodic replacement due to degradation. Consequently in this study cost of the stack has been modelled as combination of interest payments due to the initial investment and variable cost. The variable cost was calculated based on assumed stack lifetime of 80 000 h [46,49], resulting in $3 \in /MW h$. Fixed operating and maintenance (OM) costs ($C_g^{FOM,base}$) were set to $12 \in /kW/a$ [49,50] and variable operating and maintenance costs to $0.5 \in /(MW h)$ [50].

Grid connection costs and demand charges, as discussed in Section 2.2.3, must be added to these figures. Other supplementary investment costs are typically included in Lang factors [55] which may differ between technologies. As reliable values for them are not available, they are not included in this work.

2.3.2. Hydrogen storage and grid injection

Hydrogen storage may be needed to decouple the operation of electrolysis and methanation. In power-to-gas plants tank storages are preferred [56]. Investment costs from $400 \in /kg$ ($10 \in /kW h_{HHV}$) to more than $800 \in /kg$ ($20 \in /kW h_{HHV}$) have been mentioned for tank storages [57–59]. The storage pressure (300–800 bar) has an increasing effect on the investment cost [45]. In this study we use $15 \in /kW h_{HHV}$ as investment cost.

Compression work of charging the storage is calculated by the equation [60]

$$W = nZT_1 \frac{\gamma R}{\gamma - 1} N \left[\left(\frac{p_2}{p_1} \right)^{\frac{1}{N}\left(1 - \frac{1}{\gamma}\right)} - 1 \right] \qquad (17)$$

where Z is the compressibility factor, T_1 is the inlet temperature, R is the specific gas constant, n is the molar flow rate, γ is the heat capacity ratio, N is the number of stages in the compression train, p_1 is the inlet pressure and p_2 is the tank pressure. For the purpose of our model it is sufficient to linearize Eq. (17) with respect to n. Assuming an average storage pressure of 200 bar and 20 bar PEMEL output pressure we obtain energy consumption of 1.6 kW h/kg. A piston compressor is needed to

charge the storage. The compressor itself is not included in the storage cost; it requires an additional investment of $100 \in /kW_{H2,HHV}$ [59].

Small quantities of hydrogen may be allowed in the gas grid. For feeding hydrogen into the gas grid an injection station is needed. This was modelled as a separate conversion unit. Investment cost for injection station of 6.9 MW capacity, has been stated as 560 000 € [61]; study [50] assumed 75 000 € irrespective of the capacity. In this study we used $20 \in /kW_{SNG,HHV}$. Feeding into the grid is limited by the maximum allowed hydrogen concentration in natural gas, which is affected by all legacy gas consuming appliances in the grid and may range between 1 % (vol) to 10 % (vol) [62]. Here we consider the gas grid as one node where gases are perfectly mixed.

Next we consider the hydrogen concentration limit in the model. Let λ_{hyd} be the admissible energetic hydrogen fraction in the gas grid. Then we obtain the constraint

$$\left(1 - \lambda_{hyd}\right) \sum_g V_g^{hyd}(t) \leq \lambda_{hyd} \left(\sum_g V_g^{gas}(t) + max\left(V_{imp}^{gas}(t) - V_{exp}^{gas}(t), 0\right) \right) \qquad (18)$$

where V_g^{hyd} is the hydrogen feed-in by unit g, V_g^{gas} is the methane feed-in by unit g, V_{imp}^{gas} is gas import and V_{exp}^{gas} is gas export to gas transmission grid. The formula becomes nonlinear due to the fact that both V_{imp}^{gas} and V_{exp}^{gas} can assume positive values at the same time. Considering the small value of λ_{hyd}, the computational cost of adding binary variables to model Eq. (18) is excessive. To linearize the equation, we exploit the fact that gas consumption and production normally do not take place simultaneously. The approximated equation becomes

$$\left(1 - \lambda_{hyd}\right) \sum_g V_g^{hyd}(t) \leq \lambda_{hyd} \left(\sum_g V_g^{gas}(t) + \sum_g V_g^{gas,cons}(t) \right) \qquad (19)$$

where $V_g^{gas,cons}$ is the gas consumption by unit g.

2.3.3. Methanation

Methanation can transform hydrogen and CO_2 into methane by the Sabatier reaction [4]. The advantage of methanation is that methane
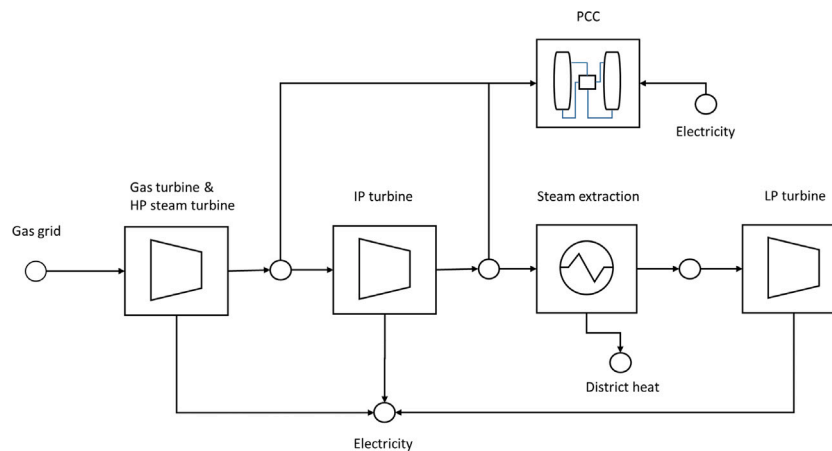
Fig. 4. Flowchart of the CHP plant and PCC steam consumption in the energy system model. The CHP unit is modelled as four conversion subunits, which convert between gas, steam, electricity and heat. PCC withdraws energy from between these subunits. The PCC also represents an electrical load.

can be fed into the gas grid without restrictions [56]. It can be seen as a way of recycling carbon. Catalytic methanation is considered here because of its suitability for large-scale operation. The methanation reaction is exothermic and the maximum chemical efficiency of conversion of hydrogen to methane is 78% [63] and that has been reached in the Etogas plant in Germany [64]. Ref. [61] uses 79.4% based on HHV. Uebbing estimated 76% based on HHV [65]. In addition, at least 10% of the input energy can be extracted as heat which is suitable for district heat supply [64,65]. Auxiliary electricity consumption for chemical methanation was estimated at most 3.8% of methane output ($0.4\,kW\,h/m^3_{SNG}$) [66] and 5.7% of methane output [65]. Here 3.8% was used. Ramp rate limit of $0.5\,\%/min$ was enforced [67].

Literature review [47] of the current investment cost of catalytic methanation revealed a wide range $140\,€/kW_{SNG,HHV}$ to $1800\,€/kW_{SNG,HHV}$. The same study estimated that by 2030 the investment cost could decrease approximately 10%. Study [61] states $1000\,€/kW_{SNG}$ in 2030. Gorre et al. estimate $375\,€/kW$ [50] for 6 MW . For injecting the product into the natural gas distribution grid, an injection station is needed. Investment cost of the station was assumed to be equal to the hydrogen injection station and was included in the methanation plant cost. Fixed O&M costs were assumed to be 5% of investment [47,50]. The variable O&M, stated as $1.1\,€/(MW\,h_{SNG})$ [50], was neglected because it is partly included in the auxiliary electricity cost.

2.3.4. CO₂ capture from flue gases

Methanation requires a source of CO_2. Ideally it should be supplied with low energetic and economic cost and adaptable flow rate [13]. Capturing and storing or utilizing CO_2 emissions (CCUS) has been discussed since 1980s [68] but lack of economic incentives as well as uncertainties related to the storage solution have prevented large-scale deployment of the technology.

While there are several technologies for CO_2 capture [69], post-combustion capture (PCC) is considered here because of its high technical maturity and wide applicability [70]. Retrofits to existing plants are possible. Commercial PCC solutions exist with monoethanolamine (MEA) as solvent. The drawback of this solution is the large amount of process heat needed for solvent regeneration [68,71]. The process heat is normally provided as steam. More than half of the steam normally entering the low pressure turbine may be required for the solvent stripper [72]. However, in case of CHP plant the waste heat produced by the PCC plant may be recovered and reused.

The model used here has been fitted to the analysis results of Laine [73] and Kärki et al. [74] of combined cycle natural gas CHP plant equipped with PCC. Fig. 4 shows the schematic layout of the PCC model in the model framework. The model assumes that the PCC draws steam from different turbine stages of the CHP plant in proportion to the processed flue gas. We note that the operation of PCC is highly flexible [75] and dynamic constraints were not set for the plant. CO_2 capture rate in current PCC designs is approximately 90%, which was also assumed in our case. However, it is also possible to increase the capture rate subject to additional costs and losses [76]. CO_2 output pressure of 20 bar was assumed.

The investment cost of the PCC plant was assumed to be $1080\,€/kg_{CO2}$, fixed annual OM costs $40\,€/kg_{CO2}$, and variable OM $5.0\,€/t_{CO2}$ [71]. In comparison study [76] gives investment cost $1170\,€/kg_{CO2}$ and the same cost for CO_2 avoided as study [71].

2.3.5. Direct air capture

CO_2 can also be captured directly from ambient air, technology known as Direct Air Capture (DAC). DAC is able to operate in distributed locations where point sources of CO_2 are not available [77]. Viebahn et al. [78] classify DAC into three subtechnologies of which they classify low-temperature DAC based on solid adsorbent as most advanced. Fasihi et al. [79] reviewed the solid adsorbent technology and projected the capital and operating costs up to 2050. They estimated the current investment cost for low-temperature DAC as $730\,€/(t/a)$ and their conservative estimate for 2030 was $338\,€/(t/a)$. The process consumes $250\,kW\,h$ to $700\,kW\,h$ electricity and $1500\,kW\,h$ to $2100\,kW\,h$ heat per tonne CO_2 at temperature of approximately 100 °C.

DAC is an emerging technology and its future costs are highly uncertain [69]. The cost estimate, which Fasihi et al. consider reliable for low-temperature DAC (their estimate for year 2020) was used in this study. Electrical consumption of $500\,kW\,h/t$ was assumed, which includes compression to output pressure 20 bar.

2.3.6. CO₂ storage

The temporal operation of SNG production may differ from that of gas consumption. This is naturally the case when the gas grid is used as energy storage. Consequently some type of CO_2 storage is needed and it can be seen as a counterpart of the grid gas storage: when gas is consumed, the CO_2 for filling the storage is available, and when SNG is fed to the grid, the CO_2 storage must be emptied. CO_2 may be stored in large quantities in liquid form in tanks or underground caverns. For tanks the conditions near the triple point (-56.6 °C, 5.2 bar) are preferred. Storage at higher pressures and temperatures is also possible but the higher cost of storage vessels offsets the savings in liquefaction and reliquefaction of boil-off gas [80,81]. The investment cost of CO_2 tanks was estimated to be $2400\,€/t_{CO2}$ [81].

Liquefaction of CO_2 can employ external or internal refrigeration. The process with external refrigeration was found most cost efficient [82]. The investment cost of the liquefaction plant was estimated
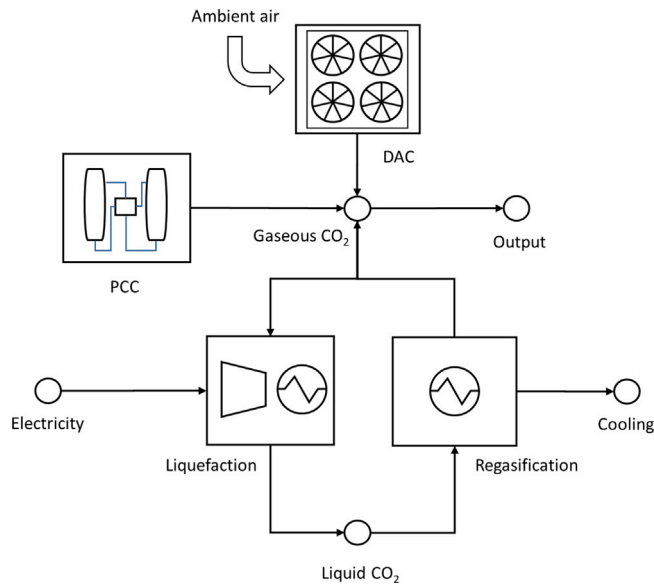
Fig. 5. Schematic of the CO_2 liquefaction process. CO_2 is supplied by PCC or DAC. For storage, it can be liquefied using electricity. The regasification process produces cooling.

as $180 \in h/kg_{CO2}$. As shown in Fig. 5, the liquefaction process consumes electricity. The electricity consumption of CO_2 liquefaction is 40 kWh/t from the inlet pressure of 20 bar [80]. Upon regasification of the liquid CO_2, approximately 100 kWh/t cooling capacity can be exploited for district cooling.

2.3.7. Distributed P2G

A separate instance of the P2G plant was placed in the LV bus as explained in Section 2.2.3. Because the main focus of the study was in the centralized P2G, the distributed P2G was modelled in a simplified manner. It included electrolysis, hydrogen storage, methanation and DAC components. The size of the hydrogen storage was fixed to 20 MW h. Due to economics of scale effects [50] the costs of the components was set higher than the centralized components, as shown in Table 2.

2.3.8. Waste heat capture and heat pumps

Capturing waste heat from different sources and recirculating it as useable heat has been considered as potential method to reduce emissions in the heat sector [83]. While a number of heat sources are possible [84], five different sources were modelled in this study. Exploiting waste water effluent is an existing practise [85]. The temperature of the waste water normally remains above 10 °C all year [86]. District cooling return water represents another source of waste heat at temperature of approximately 15 °C. Because of the similar temperature levels, these two heat sources acted as sources for a single heat pump plant in the model, which we call waste water heat pump (WWHP).

There is growing interest in exploiting deep (1 km or more) boreholes for heat collection because of their great potential: $10 \, MW/km^2$ on unobstructed land has been estimated [87,88]. We refer to the heat pumps exploiting this source as deep ground-source heat pumps (DGSHP). However, the investment cost of the borehole is high; $3700 \in /kW_{th}$ was estimated as the current cost but cost reductions are possible [88]. In this study $3000 \in /kW_{th}$ was used. The borehole temperature does not remain constant. In Finnish conditions after 10 years of operation a borehole could supply water at 8 °C [88].

Fourth possible heat source is the waste heat from the electrolysis plant. As explained in the section concerning electrolysis, it was assumed that 15% of the input energy can be extracted as heat. Finally, large-scale air-source heat pumps (ASHP) can use the ambient

Table 1
Approximation polynomial coefficients for efficiency β_{eff} and for power β_P for ASHP (Calefa Ltd. personal communication).

i	β_{eff}	β_P
0	2.54	0.5
1	0.048	0.014
2	5×10^{-4}	1.7×10^{-4}

air as heat source. They are more affordable than DGSHP but suffer from lower efficiency during cold periods. Their maximum output also strongly decreases during cold periods.

Heat pumps are needed to provide the temperature lift to normal heat supply temperatures. If Q is the thermal output, the mechanical power of the heat pump is given by [89]

$$W_{hp} = \frac{Q}{\eta_{hp}} = \frac{Q}{\psi} \left(1 - \frac{T_0}{T_{sink,out} - T_{sink,in}} ln \frac{T_{sink,out}}{T_{sink,in}} \right) \tag{20}$$

where T_0 is the heat source temperature, $T_{sink,in}$ is the temperature of the water entering the heat pump condenser, $T_{sink,out}$ is the delivery temperature of water, Q the heat output, and ψ the exergy efficiency, which depends on the heat pump design and includes motor losses. We choose $\psi = 0.50$ [90]. At 85 °C delivery temperature the resulting coefficients of performance (η_{hp}) were 3.2 and 3.0 for the waste water and ground source HP, respectively.

For the efficiency of ASHP a temperature dependent empirical polynomial function was used.

$$\frac{Q}{W_{hp}} = \sum_{i=0}^{2} \beta_{eff,i} T_{amb}^i \tag{21}$$

where T_{amb} is the ambient air temperature in Celsius. Similarly for the output capacity, which is positively correlated with T_{amb}, we use the polynomial

$$\frac{Q}{Q_0} = \sum_{i=0}^{2} \beta_{P,i} T_{amb}^i \tag{22}$$

where Q_0 is the nameplate output of the ASHP. The coefficients β have been listed in Table 1.

Heat pump delivery temperature normally cannot exceed 85 °C temperature without significant decline in efficiency [85]. In current district heating networks the supply temperature during peak load commonly exceeds this value to avoid transmission bottlenecks. In this study the supply temperature was set externally as

$$T_s(t) = a + bT_{amb}(t) \tag{23}$$

where $T_{amb}(t)$ is the ambient air temperature at time t, $a = 79.7$ °C and $b = -1.22$. In the model heat pumps were operated at maximum $T_{sink,out} = 85$ °C delivery temperature. The possible remaining temperature lift to T_s was covered by electric or gas boilers in cost optimal manner.

The investment cost of DGSHP was set to $600 \in /kW_{th}$ [90] (excluding the borehole). As the boreholes and DGSHP should be dispersed over a large area, an additional $200 \in /kW_{th}$ was allowed for the DH and electrical grid connections [91].

2.3.9. Battery energy storages

The cost of battery energy storages (BESS) has decreased in recent years and they are being considered for energy arbitrage, grid support and other applications. Here the BESS aimed at deferring transmission and distribution upgrades was modelled [92]. The battery has 6 h storage duration at maximum discharge. In Table 2 the assumed capital cost is shown in relation to discharge capacity (as opposed to energy capacity). For round-trip efficiency 86% was assumed [93].

Table 2
Financial parameters adopted for conversion and storages units.

Technology	Investment cost €/kW	Fixed OM cost €/(kW a)	Variable OM cost €/(MW h)
BESS	2100	6.9	3.6
CO₂ storage	1.0[c]	0.03	
CO₂ liquefaction	220[a]	8.8[a]	
DAC	5840[a]	x	x
Gas boilers			1.0
Gas engines	900	9.3	5
Electric boiler	60	1.0	1.0
Electrolysis	600	12	3.5
Electrolysis (distributed)	750	12	4.2
Heat pump (GSHP)	3800[d]	2	3.6
Heat pump (ASHP)	880[d]	16	3.6
Heat pump (other types)	600	2	3.6
Heat storage	4.1[b]	0.08[b]	
Hydrogen storage	15[b]	0.3	
Hydrogen compressor	100	4	
Hydrogen grid feed	20	0.2	
Methanation	580	28	
Methanation (distributed)	670	32	
Offshore wind	2500	36	2.7
PCC	1080[a]	40[a]	0.05[c]
SOFC	2000	100	1
Rooftop solar PV	800	12	

[a] €/kg$_{CO2}$/h.

[b] €/kWh.

[c] €/kg$_{CO2}$.

[d] Including grid connection.

Table 3
Technical parameters adopted for conversion units.

Unit type	Parameter	Value
CCGT	Electrical efficiency (max)	58%
	Total efficiency (max)	92%
	Start-up cost	120 €/kW
EV	Charging efficiency	90%
	Battery capacity	40 kW h
Electrolysis	Efficiency (max)	79.4 %$_{HHV}$
	Efficiency (min)	70.9 %$_{HHV}$
	Recoverable heat output	15%
Methanation	Efficiency	72
	Auxiliary elec. consumption	0.4
	Recoverable heat output	13%
	Max ramp rate	0.5 %/min
	Start-up cost	20 €/kW to 100 €/kW
	Minimum load	40%
BESS	Round-trip efficiency	86%
	Charge and discharge rate	C/6
SOFC	Electrical efficiency	60%
	Total efficiency	90%
PCC	Capture rate	90%
DAC	Heat consumption	2.0 MW h/t
	Electricity consumption	0.5 MW h/t

2.3.10. Gas to power

Direct use of hydrogen for power generation was allowed with solid oxide fuel cells (SOFC) in CHP mode. The technology is in early stage of commercialization and its cost is still high [90] (see Table 2). As an alternative power generation technology, investments into natural gas fired gas engines were possible.

2.3.11. Heat storages

Large heat storages are being constructed in Finnish DH systems. Unpressurized tank heat storages can store district heating water at temperatures below 100 °C. To maintain model linearity, the temperature of the storage was not explicitly tracked but was assumed to be high enough for discharging when the supply temperature T_s was below 95 °C. Similar to heat pumps, when T_s exceeded 95 °C, additional temperature lift by electric or gas boilers was required upon discharging. The investment cost of 4.1 €/kW h$_{th}$ [34,94] was assumed.

2.3.12. Electric vehicles

EV's can provide flexibility to the grid and can thus affect the results. The fleet of electric vehicles was modelled as a single large electricity storage with time-dependent capacity and charging constraints. The methodology was adapted from [95]. Charging efficiency of 90% was assumed [96].

2.4. Case study

To study the role of power-to-gas in reaching carbon neutrality of a city energy system, the above methodology was applied to build a model of the energy system of a medium-sized Finnish city. The purpose was not to create a detailed model of a specific city but most parameters were set according to Espoo, a city of 280,000 inhabitants in southern Finland. The city has set a goal to achieve carbon neutrality by 2030.

Rooftop area suitable for solar PV in Espoo totals 4.7 km² [97]. Availability factor of 60% was applied to this figure to account for module spacing and obstacles [98]. Using DC power density of 170 W/m² this results in total potential of 480 MW. Ground-mounted PV was not considered because of competing land uses and high price of land. Onshore wind power potential was also considered zero because of

dense inhabitation. Coastal regions in Finland generally offer good offshore wind potential. Offshore wind was included in the case study with no specific capacity upper limit. Solar PV and wind power temporal profiles for Espoo were extracted from Renewables Ninja [99]. Weather data of year 2011 was used. The average diurnal generation profiles are shown in Fig. 7. Year 2011 was chosen because the heat demand, measured by heating degree days, was slightly below the long-term average. Because of climate change, average heat demand is expected to decrease. The year accommodated also cold periods, which is required for realistic system design. Annual wind and solar power production were near the average level.

Demand profiles for electricity, district heat and cooling were not directly available for Espoo. They were estimated by fitting a linear model to the data published for a Finnish medium-sized city [100]. The explanatory variables in the model were the type of day (weekday/weekend), hour of day and ambient temperature. The model was then used to forecast demand for Espoo by scaling the total demand to the 2018 historical values [101]. The annual cooling demand was estimated based on [102]. The demand values have been listed in Table 4 and the diurnal profiles are shown in Fig. 6 The time resolution of all input time series was one hour.

Certain conversion units were assumed to be present as legacy units. These include a CCGT CHP plant (220 MW$_e$), gas boilers and WWHP. These types of plants currently exist in Espoo. New investments into these units were not allowed because the CHP plant appeared not economical; gas boilers were assumed to provide DH reserve capacity in contingencies and their capacity was thus not limited; WWHP capacity (70 MW$_{th}$) was set according to the available waste water and cooling demand. A small biogas engine (15 MW$_e$) was also present.

The initial capacity of the power transmission network connection was set based on estimated current demand as $K^0_{grid,HV} = 465$ MW$_e$. Similarly for gas transmission the capacity was set to 800 MW$_{th}$. As explained in Section 2.2.3, reinforcement investments were possible for the electrical grid. The grid reinforcement cost of the transmission grid connection $c_{grid,HV}$ is highly case specific. Based on study [103] we use 100 €/kW as base value but sensitivity analysis is done with 50 €/kW to 300 €/kW.

Connection fee for individual conversion units (e.g. heat pumps and electrolysis) to the electrical distribution grid c^{INV}_{dist} was set as 60 €/kW [61]. Capacity-based demand charge for MV grid connections was set as 20 €/(kW a), which is close to the level charged by Finnish DSO's. Time-of-use tariff was assumed for the energy fee for electricity distribution. It was set to 6 €/MW h at weekends and nights and
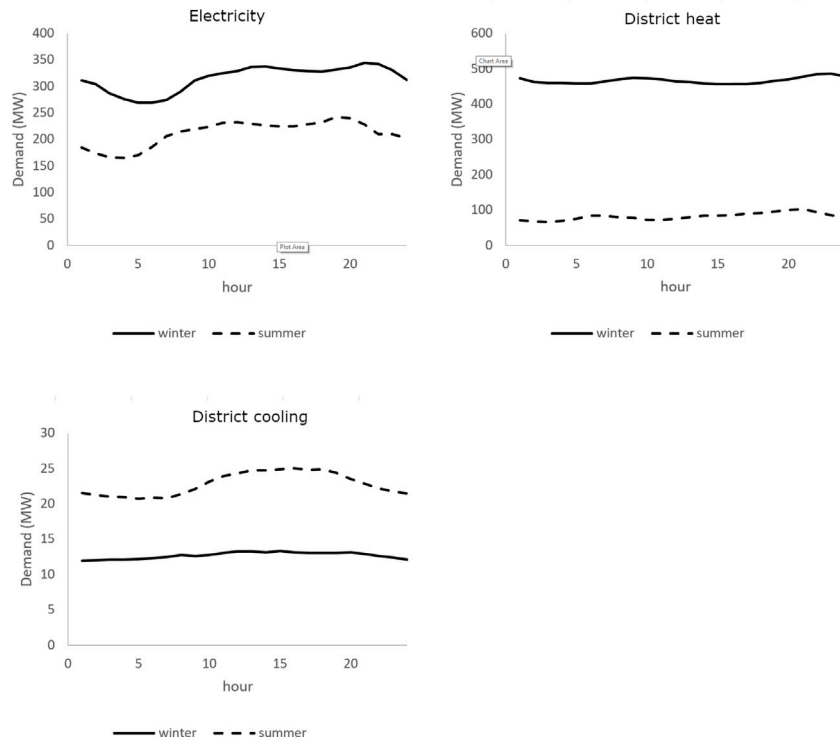
Fig. 6. Average diurnal consumption profiles of electricity, district heat and district cooling in summer and winter months.
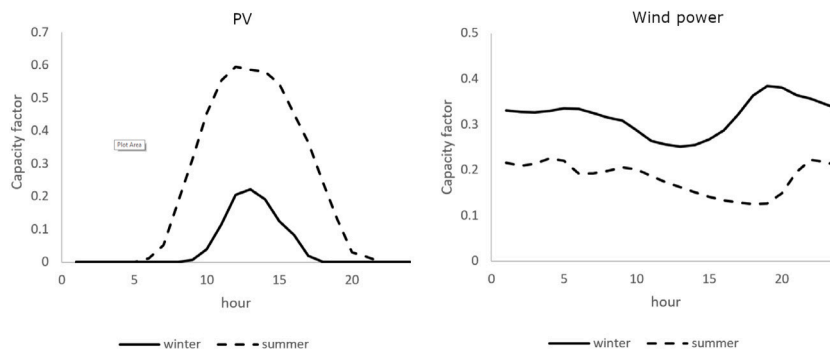

Fig. 7. Average diurnal capacity factor profiles for PV and wind power in summer and winter months.

12 €/MW h at other times. These values are based on existing tariffs. Gas transmission fee was set to 5.3 €/(MW h), which is close to current Finnish transmission tariff.

Concerning the electricity market, a scenario describing the year 2030 was built into the multinational production cost model. To be consistent, year 2011 weather data was used also in this model. The average resulting market price was 31.3 €/(MW h). The size of EV fleet was set based on the current number of EV's in Espoo and the nationwide projected number of EV's in 2030. Energy taxes or subsidies were not included in the analysis. Discount rate r was set to 6% in all scenarios [104,105].

2.5. Scenarios

Several scenarios were defined to study how P2G can contribute to the energy system to reach the carbon neutrality target. Availability of P2G was naturally chosen as one distinguishing parameter for the scenarios; availability of investments into new transmission capacity between the city and the national grid was another parameter. In the Trans scenarios the transmission capacity could be doubled to 930 MW. To study CO_2 supply, DAC availability was varied. If DAC

Table 4
Demand and price parameters used for the city in the case study.

Parameter	Value	Source
Annual electricity demand	2.1 TW h	[101]
Annual DH demand	2.0 TWh	[101]
Annual district cooling demand	150 GWh	[102]
Number of EV	19,000	
Gas price	35 €/MW h	[106]
Gas transmission charge	5.3 €/MW h	
Admissible hydrogen concentration λ_{hyd}	8.0 %vol	
Distribution demand charge c_{dist}^{FOM}	20 €/(kW a)	[107]
Distribution energy charge	6 €/MW h to 12 €/MW h	
Transmission capacity to national grid $K_{trans,0}$	465 MW	
Distribution grid reinforcement cost $c_{grid,LV}$	200 €/kW	[108]
Transmission grid reinforcement cost $c_{grid,HV}$	50 €/kW to 300 €/kW	
CO2 emission cost	60 €/t	[109]
Oxygen price	36 €/t	[110]

is not available, P2G can use a PCC plant as the CO_2 source (No DAC scenario). The purpose of the PV scenario is to study the effect of exogenously introduced small-scale PV capacity. Notice that PV

Table 5

The studied scenarios. "x" denotes that the technology is available in the scenario. The table also shows which values of relative gas usage reduction u_{gas} were studied in each scenario.

Scenario	u_{gas}	P2G	DAC	Grid reinforcement	Distributed PV	EV
Base	0–0.9	–	–	–	–	x
P2G	0–1	x	x	–	–	x
No DAC	0.97	x	–	–	–	x
Trans	1	–	–	x	–	x
Trans P2G	1	x	x	x	–	x
PV	1	x	x	x	x	x
No EV	1	x	x	x	–	–

Table 6

Optimal transmission grid reinforcement $K_{grid,HV}$ and electrolysis capacity as function of the grid reinforcement cost $c_{grid,HV}$ in two different scenarios.

Scenario	$c_{grid,HV}$ €/kW	$K_{grid,HV}$ MW	K_g^e (Electrolysis) MW
Trans P2G	50	152	13
	100	116	15
	200	82	17
	300	57	20
Trans	100	415	0

could also be activated endogenously by the investment model in any scenario. EV was present in all other scenarios except in "No EV". The scenarios are summarized in Table 5.

For each scenario different values of annual gas usage reduction u_{gas} were studied. In addition sensitivity analysis was performed with electricity market price and transmission investment cost.

2.6. Implementation

The Backbone model has been implemented on the GAMS platform. The IBM Ilog Cplex solver was used for solving the resulting MILP model. The investment model could be solved on typical laptop PC in 15 min to 3 h and the scheduling model in less than 20 min for one scenario. The integrality gap for the MILP solution was set to maximum 0.1% for the investment model and 0.01% for the scheduling model.

3. Results

3.1. Capacity investments

The Base and P2G scenarios follow the same path in terms of investments until 75% reduction in fossil gas usage (u_{gas} = 0.75) after which they diverge. Most of the investments are made in the heat sector. The air-to-water heat pump is sufficiently affordable to command 315 MW new installed capacity even when fossil gas usage is unrestricted. The capacity grows to 760 MW in the Base scenario when 90% reduction in fossil gas usage is pursued (u_{gas} = 0.9). As gas usage is reduced, the number of installed heat storages also rapidly increases. At u_{gas} = 0.9 their capacity reaches 31.2 GW h, equal to approximately one hundred typical tank storages. We find that reaching zero fossil gas usage is infeasible in the Base scenario.

Investments into different conversion and storage technologies needed for coping with the reduced fossil gas usage in these two scenarios differ mainly with P2G and heat storages. These investments are shown in Fig. 8. The abscissa shows u_{gas} as percent. In the P2G scenario P2G first enters the optimal investment portfolio at u_{gas} = 0.85. P2G is composed of electrolysis, methanation and DAC. The technologies in the Base scenario are also present in the solution, but instead of large number of heat storages the P2G scenario is able to reach the gas usage limits using P2G technology with DAC as the CO_2 source. At u_{gas} = 1, the optimal investments comprise 32 MW electrolysis, 17 MW_{gas} methanation and DAC of 3.1 t/h capacity. The absence of ASHP doubles the optimal electrolysis capacity to 63 MW and other P2G components are scaled proportionally. In this case ASHP is replaced mainly by DGSHP.

Turning to the scenarios where reinforcement of the connection to the national electricity grid is possible, grid reinforcement is not needed when fossil gas can be freely used. At u_{gas} = 1, the presence of P2G (Trans P2G scenario) clearly reduces the need of transmission capacity. As shown in Table 6, optimal grid reinforcement $K_{grid,HV}$ strongly depends on the cost $c_{grid,HV}$. There is also a positive dependency between the gas transmission cost and $K_{grid,HV}$. Compared to the P2G scenario, a smaller electrolysis plant is needed in the Trans P2G

scenario (15 MW). The optimal P2G capacity is positively correlated with grid reinforcement cost $c_{grid,HV}$ and the level of electricity price. The optimal P2G capacity weakly decreases with the gas transmission cost.

The P2G scenario without DAC (No DAC scenario) is reduced to the base scenario except at high values of u_{gas} (approximately above 0.95). In the cost optimal solution at u_{gas} = 0.97 the gas CHP is augmented with a PCC plant which can handle 58 t/h flue gas CO_2 emissions. CO_2 Storage of 12 800 t is used for seasonal storage of the captured CO_2. The P2G capacity (electrolysis of 22 MW capacity) is in line with the P2G scenario (see Fig. 9). Reaching zero fossil gas usage is infeasible also in this scenario. Because of the more costly CO_2 supply, hydrogen direct injection reaches its maximum capacity in this scenario.

Large capacity of behind-the-meter PV installations (PV scenario) thus did not change the cost optimal P2G capacity, nor did it induce investments into distributed P2G in the LV bus of our model. Similarly, the results show that the presence of EV did not have effect on the optimal P2G investments.

Investments into Rooftop PV, offshore wind power, BESS, SOFC or gas engines did not reduce total costs in any scenario.

3.2. Costs

The composition of annual costs in the Base and P2G scenarios is shown in Fig. 10. As u_{gas} increases, there are savings in gas and emission costs but the increasing cost of heat pumps, heat storages and imported electricity more than offset the savings. The total annual cost increases 13% in the P2G scenario as fossil gas use goes to zero. P2G total annual costs at u_{gas} = 1 sum to 6.6 M€ per year when the electricity cost is not included. P2G receives also direct income in the form of oxygen. At u_{gas} = 1 this amounts to 0.9 M€ per year

Cost composition of other scenarios at u_{gas} = 1 is shown in Fig. 11. The differences between the scenarios are not very large. The No DAC scenario is the most expensive one due to PCC, CO_2 storage and large number of heat storages. The category others includes electrolysis (2.0 M€), methanation (0.8 M€), CO_2 storage. Compared to the P2G scenario, the Trans P2G scenario saves in P2G and heat pump costs but suffers from higher imported electricity and grid reinforcement cost. In the Trans P2G scenario oxygen revenue amounts to 0.6 M€ per year while hydrogen direct injection only allows a cost saving of approximately 0.1 M€.

Fig. 12 summarizes the total annual cost as function of annual gas usage. The P2G scenario clearly performs better than the Base scenario at high u_{gas} values. Grid reinforcement allows a significant cost reduction and also in this case the scenario where P2G is present (Trans P2G) dominates the scenario without P2G by 3.9 M€. Notice that the Trans P2G scenario does not quite reach zero gas usage. This is because the scheduling model makes suboptimal decisions due to its aggregated time steps. We approximate the value of the additional 23 GW h gas usage using the marginal cost of gas consumption, given by the investment model (Fig. 13). Accounting for the difference in gas consumption, the annual cost difference between Trans and Trans P2G scenarios is reduced to 2.0 M€. The cost difference is increased to 4.3 M€ if the grid reinforcement cost $c_{grid,HV}$ is increased to 200 €/kW.
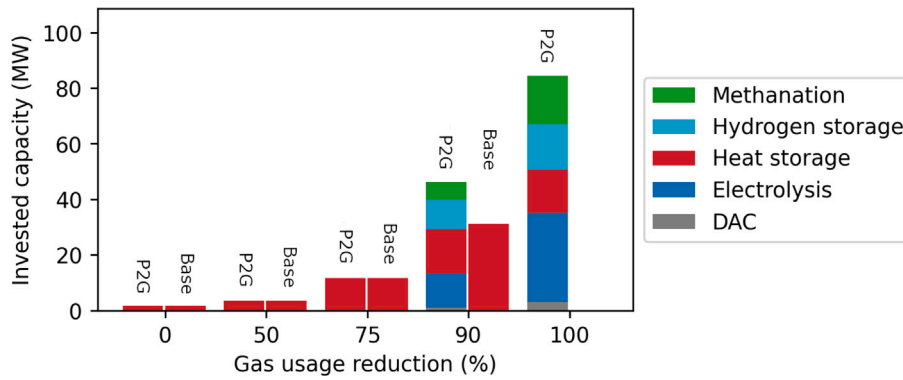
Fig. 8. Investments into selected technologies in the Base and P2G scenarios as function of gas usage limit. The numbers refer to the output capacity of units except in case of electrolysis input electrical capacity. For hydrogen storage the capacity in MWh is given and for heat storages the capacity in GWh is given.
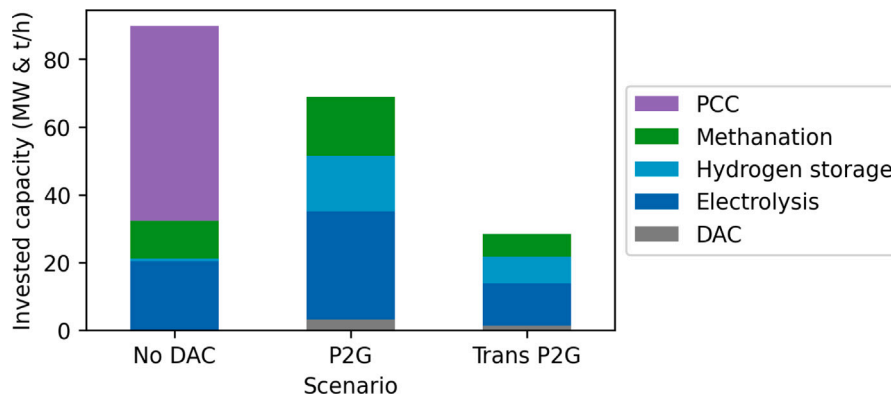

Fig. 9. Investments in the No DAC, P2G and Trans P2G scenarios when net gas usage reached its minimum (u_{gas} = 0.97 for the No DAC scenario, u_{gas} = 1 for other scenarios). For hydrogen storage the capacity in MWh is shown. For CO_2 storage the capacity is given in tens of tonnes.

The marginal cost of gas consumption, which can be obtained from the shadow price of Eq. (4), follows roughly the same pattern as the total costs. As shown in Fig. 13, in the Base scenario the marginal cost increases steeply when u_{gas} approaches 1, reflecting the fact that reaching zero gas usage is not possible. The same is true for the No DAC scenario. In the P2G scenario the marginal cost flattens when u_{gas} approaches 1 and reaches $90 \text{€}/(\text{MW h})$. Notice that this value of marginal cost assumes that the additional unit of gas is consumed within the system.

The marginal abatement cost of the measures to reduce gas usage is obtained by dividing the marginal cost of gas by the emission factor $180 \text{ kg}_{CO2}/(\text{MW h})$ (HHV). As most natural gas in Finland is of Russian origin, for the supply chain emissions we use $50 \text{ kg}_{CO2}/(\text{MW h})$ [111]. In the P2G scenario we obtain $389 \text{€}/\text{t}_{CO2}$ and for Trans P2G scenario $364 \text{€}/\text{t}_{CO2}$ at $u_{gas} = 1$.

3.3. Operation

The system mostly relied on imported electricity in all scenarios, with the exception of small amount of CHP generation at low values of u_{gas} (74 GW h, 2.7% of total demand) and in the No DAC scenario. Because SOFC did not appear cost-efficient, conversion from hydrogen to power or heat did not take place. Local VRE generation (PV) contributed only when it was exogenously specified in the PV scenario. Biogas engines produced 130 GW h in all scenarios.

The bulk of district heat was produced by ASHP and WWHP in all scenarios. As shown in Fig. 14, when fossil gas consumption was not limited, gas boilers produce approximately one quarter of all heat. Their share was diminished to 5% in the P2G scenario at $u_{gas} = 1$ and the share of ASHP increases accordingly. The contribution of waste heat from methanation and electrolysis is quite significant considering

the size of the plant, 2.5% in the P2G scenario. We note that DAC constitutes an additional heat consumer in this scenario. In the Trans scenarios the role of electric boilers is more prominent because of better electricity availability. District cooling was produced almost solely by heat pump in all scenarios, with the CO_2 regasification playing a marginal role in the No DAC scenario. Other alternatives, free cooling and compression chillers, were not economical.

Local SNG production reaches 98 GW h in the P2G scenario (capacity factor of 63% for electrolysis). As mentioned, P2G is positively correlated with electricity price in the Trans P2G scenario. This can be understood because the high electricity price makes grid reinforcement less beneficial and thus the solution of the Trans P2G scenario approaches that of the P2G scenario. Given the relatively small capacity of methanation, the gas grid capacity did not present a constraint to its operation.

Hydrogen direct injection was exploited to its maximum limit, stemming from the hydrogen concentration limit λ_{hyd}, in all scenarios involving P2G. Due to the low value of λ_{hyd}, total injection remained at maximum 3.2 GW h in the P2G scenario. Hydrogen injection capability becomes valuable during gas import periods, when according to Eq. (19) it can operate independently from methanation.

As hydrogen storage capacity remained small in all cases, its decoupling effect between electrolysis and methanation was also small. Methanation start-up cost had a clear effect on the frequency of start-ups and the hydrogen storage capacity. On reducing the start-up cost from the base value of $100 \text{€}/\text{MW}_{SNG}$ to $10 \text{€}/\text{MW}_{SNG}$, the number of start-ups increased ten-fold from 4.4 to 45 whole plant start-ups. Notice that as continuous relaxation was used for methanation online status, also certain part of the plant could be started. At the same time hydrogen storage capacity could be reduced from 16 MW h to 9 MW h.
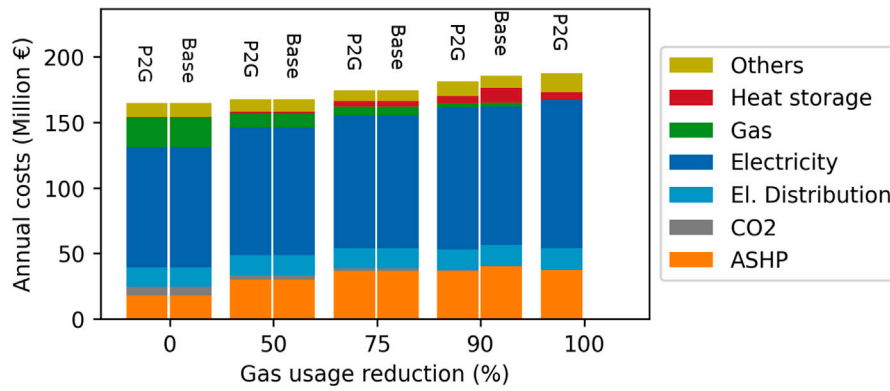
Fig. 10. Total annual costs in the Base and P2G scenarios. The category others includes e.g. electrolysis, methanation, DAC and O&M costs of gas and electric boilers. The abscissa shows the relative gas usage reduction u_{gas} in percent.
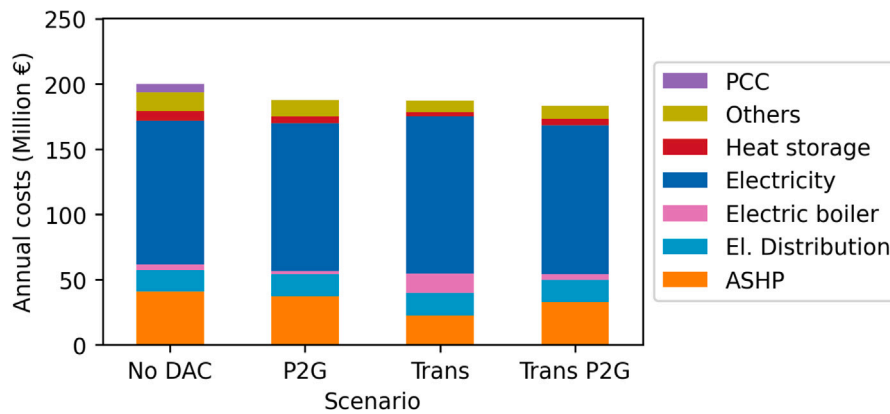

Fig. 11. Total annual costs in different scenarios when net gas usage was zero ($u_{gas} = 1$).
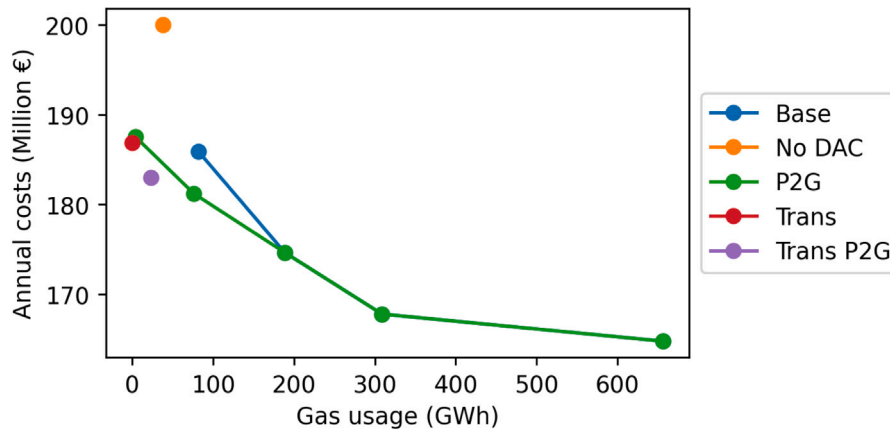

Fig. 12. Total annual costs in different scenarios as function of annual fossil gas usage. Trans, Trans P2G and No DAC scenarios are shown by points because only single very tight limit for the fossil gas usage was considered. Costs in the Base scenario and P2G scenario follow the same path (the green line) when sufficient amount of gas is available.

In scenarios involving DAC, CO_2 storage is not needed. CO_2 extraction takes place when its is needed in methanation reactor. Most of the time CO_2 presents a cost to the methanation reactor but in summer when heat is abundant, CO_2 extraction presents an economic benefit, considering the emission cost of $60 \in$/t. In the No DAC scenario the PCC must charge the long-term CO_2 storage during the short period (the peak load period) when the CHP is running. It is then discharged most of the year to keep P2G utilization factor high (Fig. 15). Unfortunately, the PCC experiences a very low utilization factor.

The absence of EV did not have effect on the optimal P2G operation. Similarly, exogenously given PV installation in the PV scenario did not have effect on the optimal P2G operation. This is understandable because the P2G plant was already operating at full power at times when PV generates power.

3.4. Accuracy of the optimization with representative slices

As explained in 2.2, for computational reasons we need to resort to approximation of the temporal axis when optimizing investments. This
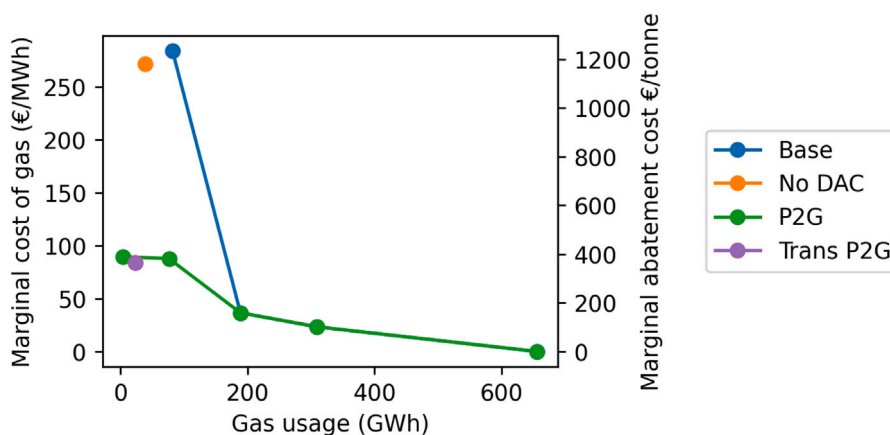
Fig. 13. Marginal cost of gas consumption in different scenarios as function of fossil gas usage in different scenarios. Marginal cost in the Base scenario and P2G scenario follow the same path (the green line) when sufficient amount of gas is available.
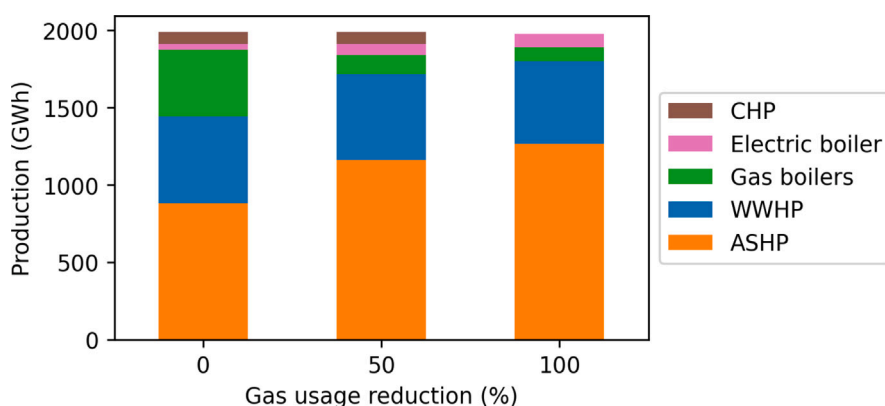

Fig. 14. District heat production in the P2G scenario as function of the gas usage limit.
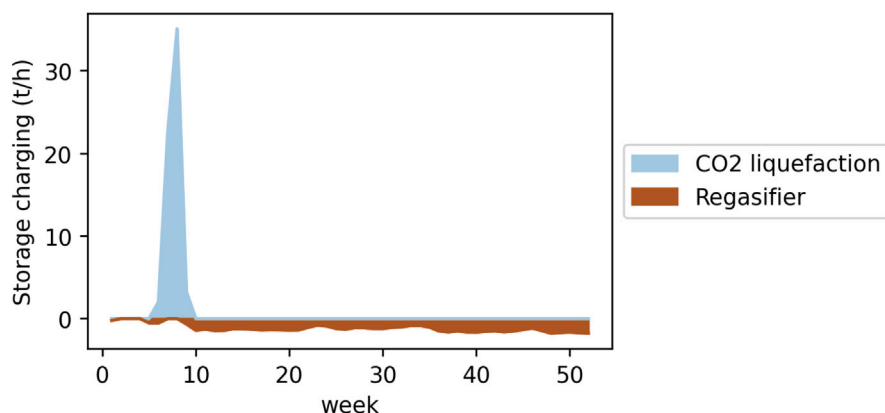

Fig. 15. CO_2 storage charging and discharging in the No DAC scenario as function of time exhibit a great deal of variation. The ordinate shows the average weekly values in tonnes per hour.

approximation is one source of error. As mentioned in Section 2.2, the results presented in literature increase our confidence on the accuracy of the results. We can obtain an estimate of lower limit of the error by running the investment model with different samples of representative slices, which are available from the random sampling process. As shows in Fig. 16, we obtain very consistent results for the optimal capacities of the main P2G components. In the Trans P2G scenario the standard deviation of optimal electrolysis and methanation capacities was 2.4 MW and 1.3 MW respectively.

4. Discussion

The results for the case study indicate that achieving the carbon neutral energy system is possible. With our assumptions of costs, available technologies and factors influencing electricity price, P2G can contribute to the cost optimal carbon neutral energy system. P2G shows economic benefits only at high emission abatement targets. Ending consumption of fossil gas altogether was not possible without investment into P2G or transmission grid expansion. The results show that exploiting P2G can help defer transmission grid expansion and allow
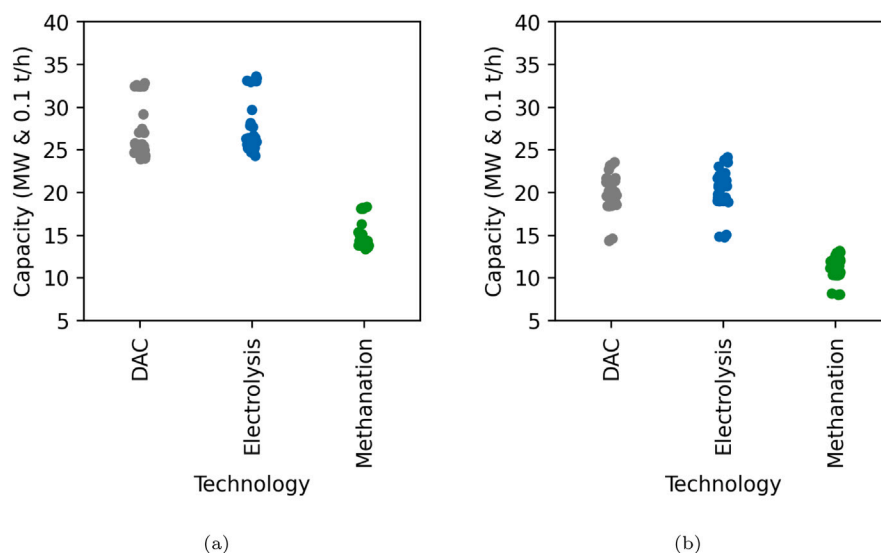
Fig. 16. Variation of the optimal investments in different technologies in the (a) P2G scenario (b) Trans P2G scenario when 30 different samples of sets of representative slices were used in the optimization. The values for DAC have been scaled so that 1 MW corresponds to 0.1 t/h.

cost savings. This is important because transmission grid reinforcement could be also limited by public opposition [112].

By adding simplified models of process components such as CO_2 capture and gas storages into the model we were able to make observations about the importance of each component. The importance of DAC is evident in the results. As DAC is independent of any CO_2 producing process, it allows great flexibility to P2G operation. When P2G was equipped with DAC, it offered great cost reductions at low emission target levels. Resorting to CO_2 capture from CHP plant flue gases is problematic. In this case P2G could contribute to cost reduction only at very low emission target levels, resulting also in very high total cost. This could be different if the CHP could profitably be operated for longer periods. The poor performance is also due to loss of CO_2 to the atmosphere, which renders zero gas usage impossible without additional sources of CO_2. The capture rate could be increased with additional costs [76], the analysis of which is an interesting topic of future study. A large CO_2 storage needs to accompany the capture plant. Approximately $6000 \, \text{m}^2$ of land would be needed for the resulting $12\,800\,\text{t}$ storage if steel tanks are used [113]. This could be a problem in tightly built sites. Storage in underground rock caverns has been envisioned but practical experience of the technology is still lacking. In addition, great attention should be paid to the potential hazards from the storage [114]

In scenarios where carbon neutrality was reached, the illustrated example city was highly dependent on imported electricity. Higher electricity prices leads to higher SNG production costs [115] and thus normally lower demand of SNG. However, when the system is dominated by electricity intensive technologies such as ASHP and electric boilers in the Trans P2G scenario, electricity price increase can have a positive effect on P2G. As P2G appears as robust investment under a range of electricity prices, the investment becomes more attractive.

Direct injection of hydrogen into the gas grid was found to be an attractive option. This can be understood as there are additional losses in the methanation process. Hydrogen concentration limits in the gas grid, however, keep the significance of direct injection from the system point of view very small. These findings are in line with [116]. However, study [116] found that because of seasonally varying gas consumption, the annual hydrogen contribution can be even lower than suggested by the concentration limit. This problem did not manifest itself in this study. A synergy appears between methanation and direct hydrogen injection. The presence of methanation, which can feed SNG into the gas grid in any proportion, supports higher electrolysis capacity, so that

the concentration limit may become the binding constraint. Hydrogen injection can also operate during gas import periods and as a result reduce the gas transmission costs. Optimal hydrogen storage capacity remained small in all scenarios. In essence, the optimization ended up with one of the strategies suggested by Gorre et al. [50] where the hydrogen storage is just large enough to compensate different ramp rates of electrolysis and methanation.

Heat pumps appear as import producers of renewable heat, which is in line with [11]. ASHP is the dominant technology; DGSHP is activated only if ASHP is not available. We can also see a connection between the DH production portfolio and optimal P2G capacity. If the portfolio consists of more expensive low-carbon technologies (DGSHP and electric boilers), larger P2G capacity is needed. Local VRE was not activated because of the fairly low electricity price. Especially for PV the problem is that grid constraints become active only in winter and PV is not available at that time.

In our scenarios the example city reached zero net usage of gas but essentially was using the gas grid as an energy storage. In the north European region there is, however, more existing gas storage capacity than what is needed in our example city per inhabitant [117]. Of course, the existing storage is needed for other functions and not all of it is available for SNG storage. The maximum withdrawal capacity of the storages may also form a limitation. In our model, some of the storage costs are included in the gas transmission tariff. If the storage capacity becomes scarce, this could be analysed by increasing the transmission tariff. Of course, if a number of cities follow the same path, the declining gas usage would also lead to an increase in the transmission tariff.

Achieving emission reductions by reducing gas usage is expensive, partly because of the low emission factor of natural gas. In the case study, the resulting emission abatement cost of more than $360 \, \text{€/t}$ is far higher than the predicted marginal abatement cost in 2030. Thus it is evident that P2G is not introduced in the mid-term without strict emission reduction goals. In 2050 however, the cost level is conceivable [118]. Some uncertainty exists about the fugitive emissions in the gas production chain [111], and somewhat lower abatement cost cannot be excluded.

The number of EV's is growing rapidly and as they present a flexible load, we hypothesized that EV's may have an effect on the optimal capacity of P2G. We see two reasons why this was not the case: Firstly, gas is mostly consumed during peak load period. EV's minimize their charging costs and thus concentrate charging periods outside of the

peak load period. Hence, they contribute rather little to the availability of power during the peak load period. Secondly, the combined storage capacity of the EV fleet in the case study was still small compared to the annual gas consumption.

The question at which level should the different energy grids interact has been presented. The presented model is suited to study the question. In the case study, we found no benefit of distributed P2G. In Nordic systems, power grids must be dimensioned according to the winter peak load, and consequently there was no congestion in the distribution grid which distributed P2G could solve. In other words, distributed P2G was in direct competition with centralized P2G, which was a more cost efficient alternative. Our assumption was that transformer backfeed does not present a problem [119].

Here we have focused on economic affordability and carbon emissions of the system. Third aspect of the energy system is security of supply [40]. From the point of view of security of supply, the P2G scenario may have positive effects because it supports the existence of the gas grid, diversifying energy supply. Security of supply was previously studied in context of integrated gas and power networks [120] but inclusion of heat demand and power-to-gas was suggested as subject of future study. In future studies, additional production forms could be included, e.g. biomass boilers, although the overall emissions of the fuel are debated [121].

5. Conclusions

Cities are trying to reach carbon neutrality. In this study, we built an investment and dispatch model for an urban energy system, which is trying to achieve carbon neutrality. The model considered both capacity investments and day-to-day operation of the system. We concentrated on a system where the main fossil fuel is natural gas. The model was applied to an example city, assuming cost and technology estimates projected for 2030. Results of the case study indicate a positive future for power-to-gas. The results are relevant also to other cities in cool climates and the published model can be used to study other locations. In future studies, the developed model can easily be extended for analysing cost-efficient decarbonization in other types of urban energy systems, as well as the system level effects of carbon neutral cities on the power system and national emission reduction costs.

CRediT authorship contribution statement

Jussi Ikäheimo: Conceptualization, Methodology, Software, Formal analysis, Writing – original draft, Writing – review & editing, Investigation, Funding acquisition. **Robert Weiss:** Conceptualization, Funding acquisition, Supervision, Investigation, Writing – original draft, Writing – review & editing, Project administration. **Juha Kiviluoma:** Methodology, Software, Funding acquisition, Supervision, Writing – review & editing. **Esa Pursiheimo:** Investigation, Conceptualization. **Tomi J. Lindroos:** Investigation, Conceptualization, Writing – review & editing.

Declaration of competing interest

The authors declare that they have no known competing financial interests or personal relationships that could have appeared to influence the work reported in this paper.

Data availability

The input data necessary for running the simulations can be accessed using the DOI doi:10.5281/zenodo.5482273. The optimization model code can be found at https://gitlab.vtt.fi/backbone/backbone.

References

[1] Masson-Delmotte V, Zhai P, Pörtner H-O, Roberts D, Skea J, Shukla PR, et al. Summary for policymakers. In: Global warming of 1.5 °C. An IPCC special report on the impacts of global warming of 1.5 °C above pre-industrial levels and related global greenhouse gas emission pathways, in the context of strengthening the global response to. IPCC-Summary for Policymakers. Geneva: World Meteorological Organization; 2018, p. 1–32. http://dx.doi.org/10.1017/CBO9781107415324.

[2] Lehtveer M, Brynolf S, Grahn M. What future for electrofuels in transport? Analysis of cost competitiveness in global climate mitigation. Environ Sci Technol 2019;53(3):1690–7. http://dx.doi.org/10.1021/acs.est.8b05243.

[3] Davis SJ, Lewis NS, Shaner M, Aggarwal S, Arent D, Azevedo IL, Benson SM, Bradley T, Brouwer J, Chiang YM, Clack CT, Cohen A, Doig S, Edmonds J, Fennell P, Field CB, Hannegan B, Hodge BM, Hoffert MI, Ingersoll E, Jaramillo P, Lackner KS, Mach KJ, Mastrandrea M, Ogden J, Peterson PF, Sanchez DL, Sperling D, Stagner J, Trancik JE, Yang CJ, Caldeira K. Net-zero emissions energy systems. Science 2018;360(6396). http://dx.doi.org/10.1126/science.aas9793.

[4] Lewandowska-Bernat A, Desideri U. Opportunities of power-to-gas technology in different energy systems architectures. Appl Energy 2018;228(May):57–67. http://dx.doi.org/10.1016/j.apenergy.2018.06.001, https://doi.org/10.1016/j.apenergy.2018.06.001.

[5] Blanco H, Faaij A. A review at the role of storage in energy systems with a focus on power to gas and long-term storage. Renew Sustain Energy Rev 2018;81(May 2017):1049–86. http://dx.doi.org/10.1016/j.rser.2017.07.062, http://dx.doi.org/10.1016/j.rser.2017.07.062.

[6] Covenant coordinators. Covenenant of Mayors action plans. 2020, https://www.covenantofmayors.eu/plans-and-actions/action-plans.html.

[7] Lund PD, Mikkola J, Ypyä J. Smart energy system design for large clean power schemes in urban areas. J Clean Prod 2015;103:437–45. http://dx.doi.org/10.1016/j.jclepro.2014.06.005.

[8] Weiss R, Saastamoinen H, Ikäheimo J, Abdurafikov R, Sihvonen T, Shemeikka J. Decarbonised district heat, electricity and synthetic renewable gas in wind- and solar-based district energy systems (in press). J Sustain Dev Energy Water Environ Syst 2021;9(2). http://dx.doi.org/10.13044/j.sdewes.d8.0340.

[9] IEA. World Energy Balances. 2019, http://dx.doi.org/10.1787/data-00512-en.

[10] Renaldi R, Friedrich D. Multiple time grids in operational optimisation of energy systems with short- and long-term thermal energy storage. Energy 2017;133:784–95. http://dx.doi.org/10.1016/j.energy.2017.05.120, http://dx.doi.org/10.1016/j.energy.2017.05.120.

[11] Salpakari J, Mikkola J, Lund PD. Improved flexibility with large-scale variable renewable power in cities through optimal demand side management and power-to-heat conversion. Energy Convers Manage 2016;126:649–61. http://dx.doi.org/10.1016/J.ENCONMAN.2016.08.041, https://www.sciencedirect.com/science/article/pii/S0196890416307154?via.

[12] Orecchini F. The era of energy vectors. Int J Hydrogen Energy 2006;31(14):1951–4. http://dx.doi.org/10.1016/j.ijhydene.2006.01.015.

[13] Schiebahn S, Grube T, Robinius M, Tietze V, Kumar B, Stolten D. Power to gas: Technological overview, systems analysis and economic assessment for a case study in Germany. Int J Hydrogen Energy 2015;40(12):4285–94. http://dx.doi.org/10.1016/j.ijhydene.2015.01.123.

[14] Fischer D, Kaufmann F, Selinger-Lutz O, Voglstätter C. Power-to-gas in a smart city context - influence of network restrictions and possible solutions using on-site storage and model predictive controls. Int J Hydrogen Energy 2018;43(20):9483–94. http://dx.doi.org/10.1016/j.ijhydene.2018.04.034.

[15] Nastasi B, Lo Basso G. Power-to-gas integration in the transition towards future urban energy systems. Int J Hydrogen Energy 2017;42(38):23933–51. http://dx.doi.org/10.1016/J.IJHYDENE.2017.07.149, https://www.sciencedirect.com/science/article/pii/S0360319917329853?_rdoc=1&_fmt=high&_origin=gateway&_docanchor=&md5=b8429449ccfc9c30159a5f9aeaa92ffb&dgcid=raven_sd_recommender_email.

[16] Zerrahn A, Schill WP. Long-run power storage requirements for high shares of renewables: review and a new model. Renew Sustain Energy Rev 2017;79:1518–34. http://dx.doi.org/10.1016/j.rser.2016.11.098.

[17] Badami M, Fambri G. Optimising energy flows and synergies between energy networks. Energy 2019;173:400–12. http://dx.doi.org/10.1016/j.energy.2019.02.007.

[18] Moeller C, Meiss J, Mueller B, Hlusiak M, Breyer C, Kastner M, Twele J. Transforming the electricity generation of the Berlin–Brandenburg region, Germany. Renew Energy 2014;72:39–50. http://dx.doi.org/10.1016/j.renene.2014.06.042.

[19] Eladl AA, El-Afifi MI, Saeed MA, El-Saadawi MM. Optimal operation of energy hubs integrated with renewable energy sources and storage devices considering CO2 emissions. Int J Electr Power Energy Syst 2020;117:105719. http://dx.doi.org/10.1016/J.IJEPES.2019.105719, https://www.sciencedirect.com/science/article/pii/S0142061519314917?via.

[20] Kötter E, Schneider L, Sehnke F, Ohnmeiss K, Schröer R. The future electric power system: Impact of power-to-gas by interacting with other renewable energy components. J Energy Storage 2016;5:113–9. http://dx.doi.org/10.1016/j.est.2015.11.012.

[21] Brandstätt C, Fette M, Meyer S. Multi-grid storage Flexibilität Für die Stromversorgung aus Gas und Wärmenetzen. Technical Report, Bremen: Fraunhofer-Institut für Fertigungstechnik und Angewandte Materialforschung IFAM; 2015, p. 119, http://www.ifam.fraunhofer.de/content/dam/ifam/de/documents/Formgebung_Funktionswerkstoffe/Energiesystemanalyse/150630-Abschlussbericht-MuGriSto-mit-Anhang.pdf.

[22] Ikäheimo J. Power-to-gas plants in a future nordic district heating system. Energy Procedia 2017;135:172–82. http://dx.doi.org/10.1016/J.EGYPRO.2017.09.500, https://www.sciencedirect.com/science/article/pii/S1876610217346039.

[23] Prasanna A, Dorer V. Feasibility of renewable hydrogen based energy supply for a district. Energy Procedia 2017;122:373–8. http://dx.doi.org/10.1016/j.egypro.2017.07.420.

[24] Berger M, Radu D, Fonteneau R, Deschuyteneer T, Detienne G, Ernst D. The role of power-to-gas and carbon capture technologies in cross-sector decarbonisation strategies. Electr Power Syst Res 2020;180(September 2019):106039. http://dx.doi.org/10.1016/j.epsr.2019.106039, https://doi.org/10.1016/j.epsr.2019.106039.

[25] Baccioli A, Bargiacchi E, Barsali S, Ciambellotti A, Fioriti D, Giglioli R, Pasini G. Cost effective power-to-x plant using carbon dioxide from a geothermal plant to increase renewable energy penetration. Energy Convers Manage 2020;226(September):113494. http://dx.doi.org/10.1016/j.enconman.2020.113494.

[26] Bailera M, Peña Bn, Lisbona P, Romeo LM. Decision-making methodology for managing photovoltaic surplus electricity through power to gas: Combined heat and power in urban buildings. Appl Energy 2018;228:1032–45. http://dx.doi.org/10.1016/J.APENERGY.2018.06.128, https://www.sciencedirect.com/science/article/pii/S0306261918309978?via.

[27] Mazzoni S, Ooi S, Nastasi B, Romagnoli A. Energy storage technologies as techno-economic parameters for master-planning and optimal dispatch in smart multi energy systems. Appl Energy 2019;254(June):113682. http://dx.doi.org/10.1016/j.apenergy.2019.113682.

[28] Beigvand SD, Abdi H, La Scala M. A general model for energy hub economic dispatch. Appl Energy 2017;190:1090–111. http://dx.doi.org/10.1016/j.apenergy.2016.12.126, http://dx.doi.org/10.1016/j.apenergy.2016.12.126.

[29] Hosseini SHR, Allahham A, Walker SL, Taylor P. Optimal planning and operation of multi-vector energy networks: A systematic review. Renew Sustain Energy Rev 2020;133(March):110216. http://dx.doi.org/10.1016/j.rser.2020.110216, https://doi.org/10.1016/j.rser.2020.110216.

[30] Sadler D, Cargill A, Crowther M, Alastair R, Watt J, Burton S, Haines M. Leeds city gate project H21. Technical Report, Northern Gas Networks; 2016, p. 382, https://www.h21.green/projects/downloads/.

[31] Helistö N, Kiviluoma J, Ikäheimo J, Rasku T, Rinne E, O'Dwyer C, Li R, Flynn D. Backbone—An adaptable energy systems modelling framework. Energies 2019;12(17):3388. http://dx.doi.org/10.3390/en12173388, https://www.mdpi.com/1996-1073/12/17/3388.

[32] Helistö N, Kiviluoma J, Holttinen H, Lara JD, Hodge BM. Including operational aspects in the planning of power systems with large amounts of variable generation: A review of modeling approaches. Wiley Interdiscip Rev 2019;8(5):1–34. http://dx.doi.org/10.1002/wene.341.

[33] Helistö N, Kiviluoma J, Reittu H. Selection of representative slices for generation expansion planning using regular decomposition. 2020, p. 23, https://cris.vtt.fi/en/publications/selection-of-representative-slices-from-historic-load-and-generat.

[34] Mansoor M, Stadler M, Zellinger M, Lichtenegger K, Auer H, Cosic A. Optimal planning of thermal energy systems in a microgrid with seasonal storage and piecewise affine cost functions. Energy 2021;215:119095. http://dx.doi.org/10.1016/j.energy.2020.119095, https://doi.org/10.1016/j.energy.2020.119095.

[35] Kotzur L, Markewitz P, Robinius M, Stolten D. Time series aggregation for energy system design: Modeling seasonal storage. Appl Energy 2018;213(January):123–35. http://dx.doi.org/10.1016/j.apenergy.2018.01.023, https://doi.org/10.1016/j.apenergy.2018.01.023.

[36] Frew BA, Jacobson MZ. Temporal and spatial tradeoffs in power system modeling with assumptions about storage: An application of the POWER model. Energy 2016;117:198–213. http://dx.doi.org/10.1016/j.energy.2016.10.074, http://dx.doi.org/10.1016/j.energy.2016.10.074.

[37] Zatti M, Gabba M, Freschini M, Rossi M, Gambarotta A, Morini M, Martelli E. K-MILP: A novel clustering approach to select typical and extreme days for multi-energy systems design optimization. Energy 2019;181:1051–63. http://dx.doi.org/10.1016/j.energy.2019.05.044, https://doi.org/10.1016/j.energy.2019.05.044.

[38] Elsido C, Bischi A, Silva P, Martelli E. Two-stage MINLP algorithm for the optimal synthesis and design of networks of CHP units. Energy 2017;121:403–26. http://dx.doi.org/10.1016/j.energy.2017.01.014, http://dx.doi.org/10.1016/j.energy.2017.01.014.

[39] Schulte Beerbühl S, Fröhling M, Schultmann F. Combined scheduling and capacity planning of electricity-based ammonia production to integrate renewable energies. European J Oper Res 2015;241(3):851–62. http://dx.doi.org/10.1016/j.ejor.2014.08.039.

[40] Heuberger CF, Staffell I, Shah N, Dowell NM. What is the value of CCS in the future energy system? Energy Procedia 2017;114:7564–72. http://dx.doi.org/10.1016/J.EGYPRO.2017.03.1888, https://www.sciencedirect.com/science/article/pii/S187661021732091X?via.

[41] Bhattacharyya S. Energy Economics - Concepts, Issues, Markets and Governance. London: Springer-Verlag; 2011, p. 721.

[42] Nolan S, Cunniffe N, Bono C, Evans M-A, Cany C, Ikäheimo J, et al. EU-SysFlex Deliverable 2.2: Scenarios and network sensitivities. Technical Report, 2018, p. 91.

[43] Fournel J, Prime G, Cunniffe N, Qazi H, Nolan S, Corcoran D, Wall P, Wasilewski J, Skwarski M, Ikäheimo J, Holttinen H, Fulgencio N, Moreira C, Silva B, Höschle H. Sysflex D2.3 - models for simulating technical scarcities on the European power system with high levels of renewable generation. Technical Report, 2018, p. 164, https://eu-sysflex.com/.

[44] Mercados. Study on tariff design for distribution systems - final report. Technical Report, EC DIRECTORATE-GENERAL FOR ENERGY; 2015, p. 652.

[45] Zhang F, Zhao P, Niu M, Maddy J. The survey of key technologies in hydrogen energy storage. Int J Hydrogen Energy 2016;41(33):14535–52. http://dx.doi.org/10.1016/j.ijhydene.2016.05.293, http://dx.doi.org/10.1016/j.ijhydene.2016.05.293.

[46] Schmidt O, Gambhir A, Staffell I, Hawkes A, Nelson J, Few S. Future cost and performance of water electrolysis: An expert elicitation study. Int J Hydrogen Energy 2017;42(52):30470–92. http://dx.doi.org/10.1016/j.ijhydene.2017.10.045, https://doi.org/10.1016/j.ijhydene.2017.10.045.

[47] Böhm H, Zauner A, Rosenfeld DC, Tichler R. Projecting cost development for future large-scale power-to-gas implementations by scaling effects. Appl Energy 2020;264:114780. http://dx.doi.org/10.1016/j.APENERGY.2020.114780, https://www.sciencedirect.com/science/article/pii/S0306261920302920?via.

[48] Buttler A, Spliethoff H. Current status of water electrolysis for energy storage, grid balancing and sector coupling via power-to-gas and power-to-liquids: A review. Renew Sustain Energy Rev 2018;82(February 2017):2440–54. http://dx.doi.org/10.1016/j.rser.2017.09.003.

[49] Bertuccioli L, Chan A, Hart D, Lehner F, Madden B, Standen E. Development of water electrolysis in the European union - final report. Technical Report, (February):E4tech Sàrl with Element Energy Ltd; 2014, p. 160, http://www.fch-ju.eu/sites/default/files/studyelectrolyser_0-Logos_0_0.pdf.

[50] Gorre J, Ortloff F, van Leeuwen C. Production costs for synthetic methane in 2030 and 2050 of an optimized power-to-gas plant with intermediate hydrogen storage. Appl Energy 2019;253:113594. http://dx.doi.org/10.1016/J.APENERGY.2019.113594, https://www.sciencedirect.com/science/article/pii/S0306261919312681.

[51] Nieminen J, Dincer I, Naterer G. Comparative performance analysis of PEM and solid oxide steam electrolysers. Int J Hydrogen Energy 2010;35(20):10842–50. http://dx.doi.org/10.1016/j.ijhydene.2010.06.005, http://dx.doi.org/10.1016/j.ijhydene.2010.06.005.

[52] Saba SM, Müller M, Robinius M, Stolten D. The investment costs of electrolysis – A comparison of cost studies from the past 30 years. Int J Hydrogen Energy 2018;43(3):1209–23. http://dx.doi.org/10.1016/j.ijhydene.2017.11.115.

[53] Gaul A, Bohn U. Power-to-Gas demonstration plant Ibbenbüren. Technical Report, (November). 2015, http://dx.doi.org/10.13140/RG.2.1.3069.1288.

[54] Hinkley J, Hayward J, Mcnaughton R, Gillespie R, Matsumoto A, Watt M, Lovegrove K. Cost assessment of hydrogen production from PV and electrolysis. Technical Report, CSIRO; 2016, p. 1–35, http://arena.gov.au/files/2016/05/Assessment-of-the-cost-of-hydrogen-from-PV.pdf.

[55] van Amsterdam M. Factorial techniques applied in chemical plant cost estimation : A comparative study based on literature and cases. (Ph.D. thesis), Delft University of Technology; 2018, p. 158.

[56] Gahleitner G. Hydrogen from renewable electricity : An international review of power-to-gas pilot plants for stationary applications. Int J Hydrogen Energy 2012;38(5):2039–61. http://dx.doi.org/10.1016/j.ijhydene.2012.12.010.

[57] Schoenung S. Economic analysis of large-scale hydrogen storage for renewable utility applications. In: Sandia Report. Albuquerque: Sandia National Laboratories; 2011, p. 41, http://prod.sandia.gov/techlib/access-control.cgi/2011/114845.pdf.

[58] Wang Y, Kowal J, Leuthold M, Sauer DU. Storage system of renewable energy generated hydrogen for chemical industry. Energy Procedia 2012;29:657–67. http://dx.doi.org/10.1016/j.egypro.2012.09.076, http://dx.doi.org/10.1016/j.egypro.2012.09.076.

[59] Grond L, Schulze P, Holstein J. Systems analyses power to gas; deliverable 1: Technology review. In: Project Systems Analyses Power-To-Gas Pathways. Technical Report, GCS 13.R.2, Groningen: DNV Kema; 2013, p. 1–70.

[60] Nederstigt P. Real gas thermodynamics and the isentropic behavior of substances. (Ph.D. thesis), Delft University of Technology; 2017, p. 112.

[61] ENEA Consulting. The Potential of Power-To-Gas. vol. 33, 2016, p. 51.

[62] Altfeld K, Pinchbeck D. Admissible hydrogen concentrations in natural gas systems. Gas for Energy 2013;March/2013:1–16, www.gas-for-energy.com.

[63] Götz M, Lefebvre J, Mörs F, McDaniel Koch A, Graf F, Bajohr S, Reimert R, Kolb T. Renewable power-to-gas: A technological and economic review. Renew Energy 2016;85:1371–90. http://dx.doi.org/10.1016/j.renene.2015.07. 066, http://linkinghub.elsevier.com/retrieve/pii/S0960148115301610.

[64] Sveinbjörnsson D, Munster E. Upgrading of biogas to biomethane with the addition of hydrogen from electrolysis. In: Future Gas Deliverable D1.1.1. Technical Report, Planenergi; 2017, p. 1–28.

[65] Uebbing J, Rihko-Struckmann LK, Sundmacher K. Exergetic assessment of CO2 methanation processes for the chemical storage of renewable energies. Appl Energy 2019;233–234(September 2018):271–82. http://dx.doi.org/10.1016/j. apenergy.2018.10.014, https://doi.org/10.1016/j.apenergy.2018.10.014.

[66] Götz M, Koch AMD, Graf F. State of the art and perspectives of CO2 methanation process concepts for power-to-gas applications. In: Int Gas Res Conf Proc. 1, (January):Copenhagen; 2014, p. 314–27.

[67] Aicher T, Iglesias-Gonzales M, Götz M. Arbeitspaket 5 : Betrachtungen des gesamtsystems im hinblick auf dynamik und prozessintegration. Energie Wasser Prax 2014;(January 2014):51–5, https://www.researchgate.net/publication/ 272488412_Arbeitspaket_5_Betrachtungen_des_Gesamtsystems_im_Hinblick_auf_ Dynamik_und_Prozessintegration.

[68] Oexmann J, Hensel C, Kather A. Post-combustion CO2-capture from coal-fired power plants: Preliminary evaluation of an integrated chemical absorption process with piperazine-promoted potassium carbonate. Int J Greenh Gas Control 2008;2(4):539–52. http://dx.doi.org/10.1016/j.ijggc.2008.04.002.

[69] IEA. Energy technology perspectives special report on carbon capture utilisation and storage. In: Energy Technology Perspectives. Technical Report, 2020, p. 169. http://dx.doi.org/10.1787/9789264109834-en.

[70] Hu Y, Gao Y, Lv H, Xu G, Dong S. A new integration system for natural gas combined cycle power plants with CO2 capture and heat supply. Energies 2018;11(11). http://dx.doi.org/10.3390/en11113055.

[71] Li K, Leigh W, Feron P, Yu H, Tade M. Systematic study of aqueous mo-noethanolamine (MEA) -based CO 2 capture process : Techno-economic assessment of the MEA process and its improvements. Appl Energy 2016;165:648–59. http://dx.doi.org/10.1016/j.apenergy.2015.12.109, http://dx.doi.org/10.1016/ j.apenergy.2015.12.109.

[72] Xu G, Wu Y, Yang Y, Zhang K, Song X. A novel integrated system with power generation, CO2 capture, and heat supply. Appl Therm Eng 2013;61(2):110–20. http://dx.doi.org/10.1016/J.APPLTHERMALENG.2013.07. 016, https://www.sciencedirect.com/science/article/pii/S1359431113005048? via.

[73] Laine M. Effects of carbon capture on an existing combined cycle gas turbine power plant. (Ph.D. thesis), Aalto University; 2011, p. 63.

[74] Kärki J, Tsupari E, Arasto A. CCS Feasibility improvement in industrial and municipal applications by heat utilisation. Energy Procedia 2013;37:2611–21. http://dx.doi.org/10.1016/J.EGYPRO.2013.06.145, https://www.sciencedirect. com/science/article/pii/S1876610213003883?via.

[75] Ceccarelli N, van Leeuwen M, Wolf T, van Leeuwen P, van der Vaart R, Maas W, Ramos A. Flexibility of low-CO2 gas power plants: Integration of the CO2 capture unit with CCGT operation. Energy Procedia 2014;63:1703–26. http: //dx.doi.org/10.1016/J.EGYPRO.2014.11.179, https://www.sciencedirect.com/ science/article/pii/S1876610214019948.

[76] IEAGHG. Towards zero emissions CCS in power plants using higher capture rates or biomass. Technical Report, (March):IEA; 2019, p. 1–128, http:// documents.ieaghg.org/index.php/s/CLIZIvBI6OdMFnf/download.

[77] Lackner K. Capture of carbon dioxide from ambient air. Eur Phys J Special Top 2009;176(1):93–106. http://dx.doi.org/10.1140/epjst/e2009-01150-3.

[78] Viebahn P, Scholz A, Zelt O. The potential role of direct air capture in the german energy research program — Results of a multi-dimensional analysis. Energies 2019;(Special Issue Multicriteria Assessment and Derivation of R&D Recommendations for Low-Carbon Energy Technologies—Selected Papers from the Research Study "Technologies for the Energy Transition).

[79] Fasihi M, Efimova O, Breyer C. Techno-economic assessment of CO 2 direct air capture plants. J Clean Prod 2019;224(April):957–80. http://dx.doi.org/10. 1016/j.jclepro.2019.03.086.

[80] Aspelund A, Mølnvik M, De Koeijer G. Ship transport of CO2: Techni-cal solutions and analysis of costs, energy utilization, exergy efficiency and CO2 emissions. Chem Eng Res Des 2006;84(9):847–55. http://dx.doi. org/10.1205/CHERD.5147, https://www.sciencedirect.com/science/article/pii/ S0263876206729665.

[81] Kujanpää L, Ritola J, Nordbäck N, Teir S. Scenarios and new technologies for a north-European CO2 transport infrastructure in 2050. Energy Procedia 2014;63:2738–56. http://dx.doi.org/10.1016/j.egypro.2014.11.297, http://dx. doi.org/10.1016/j.egypro.2014.11.297.

[82] Øi LE, Eldrup N, Adhikari U, Bentsen MH, Badalge JL, Yang S. Simulation and cost comparison of CO2 liquefaction. Energy Procedia 2016;86(1876):500– 10. http://dx.doi.org/10.1016/j.egypro.2016.01.051, http://dx.doi.org/10. 1016/j.egypro.2016.01.051 http://ac.els-cdn.com/S1876610216000539/1- s2.0-S1876610216000539-main.pdf?_tid=2cf34838-e3d4-11e6-a874- 00000aacb35d&acdnat=1485441290_c8cd628dd282fe8c0bc06552ce0d1d91.

[83] Arabzadeh V, Mikkola J, Jasiūnas J, Lund PD. Deep decarbonization of urban energy systems through renewable energy and sector-coupling flexibility strategies. J Environ Manage 2020;260(November 2019). http://dx.doi.org/10. 1016/j.jenvman.2020.110090.

[84] Lund R, Persson U. Mapping of potential heat sources for heat pumps for district heating in Denmark. Energy 2016;110:129–38. http://dx.doi.org/10. 1016/j.energy.2015.12.127, http://dx.doi.org/10.1016/j.energy.2015.12.127.

[85] Valor Partners. Suuret lämpöpumput kaukolämpöjärjestelmässä: Loppuraportti. In: Technical Report. Finnish Energy Industries; 2016, p. 50, https: //energia.fi/files/993/Suuret_lampopumput_kaukolampojarjestelmassa_ Loppuraportti_290816_paivitetty.pdf.

[86] Luhtaniemi S. Lämpötilan vaikutus aktiivilieteprosessin toimintaan ja ohjauk-seen. (Ph.D. thesis), University of Oulu; 2017, p. 41.

[87] Wennerström M, Sallasmaa O, Witick I, Korhonen K, Kallio J. Helsingin geo-energiapotentiaali. In: Technical Report. Geological Survey of Finland; 2019, p. 94.

[88] Pentti E, Tiensuu K. Planetaarista kaukolämpöä tarjolla – rajattomasti ja halvalla? In: Technical Report. AFRY; 2019, p. 3.

[89] Ertesvåg IS. Uncertainties in heat-pump coefficient of performance (COP) and exergy efficiency based on standardized testing. Energy Build 2011;43(8):1937–46. http://dx.doi.org/10.1016/J.ENBUILD.2011.03.039, https://www.sciencedirect.com/science/article/pii/S0378778811001484.

[90] Danish Energy Agency. Technology data for energy plants for electricity and district heating generation - Feb. 2019. In: Technical Report. 2019.

[91] Sihvola V. Teollisuuden hukkalämmön hyödyntäminen kaukolämpöverkossa. (Ph.D. thesis), Jyväskylä University of Applied Sciences; 2019, p. 59, http: //urn.fi/URN:NBN:fi:amk-2019053113857.

[92] Lazard. LAZARD'S LEVELIZED COST OF STORAGE ANALYSIS V5.0. In: Technical Report. 2019, p. 47.

[93] Zakeri B, Syri S. Electrical energy storage systems: A comparative life cycle cost analysis. Renew Sustain Energy Rev 2015;42:569–96. http://dx.doi.org/ 10.1016/j.rser.2014.10.011, http://dx.doi.org/10.1016/j.rser.2014.10.011.

[94] Schmidt T, Miedaner O. Solar district heating guidelines - Storage. Technical Report, 2012, p. 1–13, http://solar-district-heating.eu/Portals/0/Factsheets/ SDH-WP3_FS-7-2_Storage_version3.pdf.

[95] Kiviluoma J, Meibom P. Methodology for modelling plug-in electric vehicles in the power system and cost estimates for a system with either smart or dumb electric vehicles. Energy 2011;36:1758–67.

[96] Kieldsen A, Thingvad A, Martinenas S, Srensen TM. Efficiency test method for electric vehicle chargers, In: EVS 2016 - 29th International Electric Vehicle Symposium, 2016.

[97] Helsingin seudun ympäristöpalvelut HSY. Suitable areas for solar panels in helsinki region. 2016, https://hri.fi.

[98] Bódis K, Kougias I, Jäger-Waldau A, Taylor N, Szabó S. A high-resolution geospatial assessment of the rooftop solar photovoltaic potential in the Euro-pean union. Renew Sustain Energy Rev 2019;114:109309. http://dx.doi.org/10. 1016/J.RSER.2019.109309, https://www.sciencedirect.com/science/article/pii/ S1364032119305179.

[99] Pfenninger S, Staffell I. Long-term patterns of European PV output us-ing 30 years of validated hourly reanalysis and satellite data. Energy 2016;114:1251–65. http://dx.doi.org/10.1016/j.energy.2016.08.060, http://dx. doi.org/10.1016/j.energy.2016.08.060.

[100] Sähkölaitos T. Energy consumption in tampere. 2020, https://www.sahkolaitos. fi/aina-apuna/kulutus-tampereella/.

[101] seudun ympäristöpalvelut HSY H. Energy Consumption in the Helsinki Metropolitan Area. Helsingin seudun ympäristöpalvelut HSY; 2019, http:// www.hsy.fi/avoindata.

[102] Nuutinen T. Kaukojäähdytys vanhoissa asuinkerrostaloissa. (Ph.D. thesis), Metropolia University of Applied Sciences; 2015, p. 50, http://urn.fi/URN:NBN: fi:amk-201505219412.

[103] Mutale J, Strbac G. Transmission network reinforcement versus FACTS: an economic assessment. IEEE Trans Power Syst 2000;15(3):961–7. http://dx.doi. org/10.1109/59.871719.

[104] Clack CTM, Qvist SA, Apt J, Bazilian M, Brandt AR, Caldeira K, Davis SJ, Diakov V, Handschy MA, Hines PD, Jaramillo P, Kammen DM, Long JC, Morgan MG, Reed A, Sivaram V, Sweeney J, Tynan GR, Victor DG, Weyant JP, Whitacre JF. Evaluation of a proposal for reliable low-cost grid power with 100% wind, water, and solar. Proc Natl Acad Sci 2017;114(26):6722–7. http: //dx.doi.org/10.1073/pnas.1610381114, http://www.pnas.org/lookup/doi/10. 1073/pnas.1610381114.

[105] LLP GTU. Renewable energy discount rate survey results – 2018. Technical Report, Grant Thornton UK LLP; 2019, p. 28, https://www.grantthornton.co. uk/globalassets/1.-member-firms/united-kingdom/pdf/documents/renewable- energy-discount-rate-survey-results-2018.pdf.

[106] Duic N, Stefanic N, Lulic Z, Krajacic G, Puksec T, Novosel T. Heat roadmap europe deliverable 6.1: Future fuel price review. Technical Report, 2017, p. 40, https://heatroadmap.eu/.

[107] Ikäheimo J, Jones M, Naberezhnykh D, Garcia A, Canet Sabate M. Zeeus deliverable 55.5: Business cases for bus fleet charging operator at depot. Technical Report, 2018, p. 54.

[108] Tuunanen J, Valtonen P, Honkapuro S, Partanen J. A general investigation about how to divide DR benefits between DSO and markets. In: International Conference on the European Energy Market, EEM, 2016, p. 5. http://dx.doi.org/10.1109/EEM.2016.7521306.

[109] European Network of Transmission System Operators for Electricity (ENTSO-E). TYNDP 2020 scenario report. Technical Report, ENTSO-E; 2020, p. 64, http://www.entsoe.eu.

[110] Hurskainen M. Industrial oxygen demand in Finland. Technical Report, VTT Technical Research Centre of Finland; 2017, p. 22, https://cris.vtt.fi/.

[111] Muller-Syring G, Große C, Eysser M, Glandien J, Schütz S. Critical evaluation of default values for the GHG emissions of the natural gas supply chain. In: International Gas Research Conference Proceedings. Technical Report, Berlin: DBI Gas- und Umwelttechnik GmbH; 2017, p. 102.

[112] Battaglini A, Komendantova N, Brtnik P, Patt A. Perception of barriers for expansion of electricity grids in the European union. Energy Policy 2012;47:254–9. http://dx.doi.org/10.1016/j.enpol.2012.04.065, https://linkinghub.elsevier.com/retrieve/pii/S0301421512003709.

[113] Ritola J, Lindberg A, Kujanpää L, Nordbäck N. CLEEN - CCS Task 4 . 21 CO2 - terminals and intermediate storage - final report 2013. Technical Report, Helsinki, Finland: Cleen oy; 2014, p. 48, www.vtt.fi.

[114] IEA Greenhouse Gas R&D Programme. Safety in carbon dioxide capture, transport and storage.. Technical Report, IEA GHG; 2009, p. 137.

[115] Vandewalle J, Bruninx K, D'haeseleer W. Effects of large-scale power to gas conversion on the power, gas and carbon sectors and their interactions. Energy Convers Manage 2015;94:28–39. http://dx.doi.org/10.1016/j.enconman.2015.01.038, http://linkinghub.elsevier.com/retrieve/pii/S0196890415000424.

[116] Simonis B, Newborough M. Sizing and operating power-to-gas systems to absorb excess renewable electricity. Int J Hydrogen Energy 2017;42(34):21635–47. http://dx.doi.org/10.1016/J.IJHYDENE.2017.07.121, https://www.sciencedirect.com/science/article/pii/S0360319917329506?via.

[117] Ramboll Oil and Gas. Study on natural gas storage in the EU study on natural storage in the EU. Technical Report, Directorate-General for Mobility and Transport (European Commission); 2008, p. 339.

[118] Blanco H, Nijs W, Ruf J, Faaij A. Potential of power-to-methane in the EU energy transition to a low carbon system using cost optimization. Appl Energy 2018;232:323–40. http://dx.doi.org/10.1016/J.APENERGY.2018.08.027, https://www.sciencedirect.com/science/article/pii/S0306261918311826.

[119] Mack R, Sakib M, Succar S. Impacts of substation transformer backfeed at high PV penetrations. In: 2017 IEEE Power & Energy Society General Meeting. IEEE; 2017, p. 1–5. http://dx.doi.org/10.1109/PESGM.2017.8274081, http://ieeexplore.ieee.org/document/8274081/.

[120] Qiu J, Dong ZY, Zhao JH, Meng K, Zheng Y, Hill DJ. Low carbon oriented expansion planning of integrated gas and power systems. IEEE Trans Power Syst 2015;30(2):1035–46. http://dx.doi.org/10.1109/TPWRS.2014.2369011.

[121] Luyssaert S, Marie G, Valade A, Chen Y-Y, Njakou Djomo S, Ryder J, Otto J, Naudts K, Lansø AS, Ghattas J, McGrath MJ. Trade-offs in using European forests to meet climate objectives. Nature 2018;562(7726):259–62. http://dx.doi.org/10.1038/s41586-018-0577-1.